Published in final edited form as:
Sci Transl Med. 2024 January 17; 16(730): eadi9711. doi:10.1126/scitranslmed.adi9711.

Commensal Antimicrobial Resistance Mediates Microbiome Resilience to Antibiotic Disruption

Shakti K Bhattarai[1,2], **Muxue Du**[3,4], **Abigail L Zeamer**[1,2], **Benedikt M Morzfeld**[1,2], **Tasia D Kellogg**[1,2], **Kaya Firat**[5], **Anna Benjamin**[3], **James M Bean**[3], **Matthew Zimmerman**[5], **Gertrude Mardi**[6], **Stalz Charles Vilbrun**[6], **Kathleen F Walsh**[7,8], **Daniel W Fitzgerald**[7], **Michael S Glickman**[3,4,*], **Vanni Bucci**[1,2,9,*]

[1]Department of Microbiology and Physiological Systems, UMass Chan Medical School, Worcester, MA 01605, USA.

[2]Program in Microbiome Dynamics, UMass Chan Medical School, Worcester, MA 01605, USA.

[3]Immunology Program, Memorial Sloan Kettering Cancer Center, New York, NY 10065, USA.

[4]Immunology and Microbial Pathogenesis Graduate Program, Weill Cornell Graduate School, New York, NY 10065, USA.

[5]Center for Discovery and Innovation, Hackensack Meridian Health, Nutley, NJ 07110, USA.

[6]Haitian Study Group for Kaposi's Sarcoma and Opportunistic Infections (GHESKIO), Port-au-Prince, Haiti.

[7]Center for Global Health, Weill Cornell Medicine, New York, NY 10065, USA.

[8]Division of General Internal Medicine, Weill Cornell Medicine, New York, NY 10065, USA.

[9]Immunology and Microbiology Program, UMass Chan Medical School, Worcester, MA 01605, USA.

[*]Correspondence to: glickmam@mskcc.org, vanni.bucci@umassmed.edu.

Author Contributions:
The study was conceptualized by MSG, DWF, and VB. DWF, SCV, GM, and KFW were responsible for patient recruitment, enrollment, and sample collection. MD, AB, and MSG processed stool samples to prepare DNA. JB was responsible for informatics for sample tracking and sample tracking and verification. AZ, TK, BM performed microbiome sequencing and animal experimentation. MZ and KF analyzed antibiotic levels in stool. SKB, VB, and MSG performed data analysis and interpretation. Overall supervision for the study was provided by MSG and VB with VB and MSG writing the initial draft of the manuscript and all authors editing.

Competing interests:
MSG reports consulting fees and equity in Vedanta Biosciences, Inc., consulting fees from Fimbrion Therapeutics. VB reports consulting fees Vedanta Biosciences, Inc. The remaining authors declare that they have no competing interests.

Data and materials availability:
All data associated with this study are in the paper or supplementary materials. Microbiome sequencing data and peripheral blood transcriptomic data are deposited in the SRA with accession number PRJNA1025016. Data file S3 is available at https://doi.org/10.6084/m9.figshare.24082575.v1. Code to perform all the reported analysis is available in Zenodo at (96).

Overline: GUT MICROBIOME

List of supplementary materials
Materials and Methods
Figures S1 to S7
MDAR checklist
Data files S1-S3

Abstract

Despite their therapeutic benefits, antibiotics exert collateral damage on the microbiome and promote antimicrobial resistance. However, the mechanisms governing microbiome recovery from antibiotics are poorly understood. Treatment of *Mycobacterium tuberculosis*, the world's most common infection, represents the longest antimicrobial exposure in humans. Here, we investigate gut microbiome dynamics over 20 months of multi-drug-resistant tuberculosis and 6 months of drug-sensitive tuberculosis (TB) treatment in humans. We find that gut microbiome dynamics and TB clearance are shared predictive cofactors of the resolution of TB-driven inflammation. The initial severe taxonomic and functional microbiome disruption, pathobiont domination, and enhancement of antibiotic resistance that initially accompanied long-term antibiotics was countered by later recovery of commensals. This resilience was driven by the competing evolution of antimicrobial resistance mutations in pathobionts and commensals, with commensal strains with resistance mutations reestablishing dominance. Fecal-microbiota transplantation of the antibiotic-resistant commensal microbiome in mice recapitulated resistance to further antibiotic disruption. These findings demonstrate that antimicrobial resistance mutations in commensals can have paradoxically beneficial effects by promoting microbiome resilience to antimicrobials and identify microbiome dynamics as a predictor of disease resolution in antibiotic therapy of a chronic infection.

One sentence summary:

The gut microbiome evolves under antibiotic pressure, allowing healthy commensals to outcompete pathobionts and reestablish a healthy microbiome.

Introduction

Short courses of broad-spectrum antibiotics dramatically perturb the healthy gastrointestinal (GI) microbiome in both adults and children(1–3), with the present understanding that during treatment, the microbiome is locked into an alternative stable state that lasts well past treatment cessation(4–7). Antibiotic-induced dysbiosis is characterized by the enrichment of pro-inflammatory communities, GI distress including diarrhea(8), exacerbation of inflammatory pathways, and impaired colonization resistance against pathogens(9, 10). Additionally, antibiotics enrich for antibiotic resistance genes (ARGs) in the microbiome (known as the GI resistome)(2) which has been linked to greater incidence of extra-intestinal infections from multi-drug and extensively-drug resistant bacteria(11).

As for other microbial ecological systems responding to short-term perturbations(12), return of the microbiome to the pre-treatment state after antibiotics depends on the relative fitness of the dominant pathobionts and the depleted commensals(13). Although both theoretical work(7) and recent studies in animals(14) demonstrate that microbiome recovery varies as a function of the type of antibiotic, networks of microbial interaction, diet, and proximity to environmental bacterial reservoirs, the ultimate determinants of this resilience are unknown. A recent study profiling the microbiome of a single individual found that although antibiotics can drive rapid shifts in the genetic composition of individual commensal species, these changes reverted to baseline once antibiotic treatment had concluded(15). However,

longer antibiotic perturbations may stimulate distinct adaptive mechanisms, especially considering that the genomic analysis of microbiome long-term dynamics (months—years) in healthy individuals shows that the microbiome undergoes genetic adaptation even in the absence of external perturbations (16, 17). Additionally, given the influence of antibiotic-dependent changes in the microbiome on immunity(18), it is plausible that adaptation of resident commensals to prolonged antibiotics might impact the treatment outcome for chronic infections in which host immunity is an important cofactor.

Here we investigate how the gut microbiome adapts to prolonged antibiotic therapy and how this adaptation influences infection-driven inflammatory responses. We focus on multidrug-resistant (MDR) tuberculosis (TB) treatment, which involves the longest antibiotic exposure in humans, lasting around 20 months(19). Treating TB requires combinations of antibiotics with broader antimicrobial activity compared to standard TB therapy(20), yet the effect of MDR TB treatment on microbiome composition is unknown. Our findings directly support the notion that microbiome resilience can occur through commensal antimicrobial resistance and that microbiome dynamics may play a role in regulating peripheral immune responses during long-term antibiotic treatment for MDR TB.

Results

MDR TB treatment severely disrupts stool taxonomic and functional composition of the microbiome

We recently described the effect of standard TB therapy on microbial species abundance and built computational models that implicate microbiome-dependent effects on TB disease activity(21). Here, we sought to extend these studies to the treatment of MDR TB, which is longer in duration and uses broader-spectrum antibiotics. We enrolled 24 individuals (13 males and 11 females) with MDR TB who were initiating therapy, most of whom had failed prior standard treatment, commonly referred to as HRZE (consisting of isoniazid, rifampin, pyrazinamide, ethambutol). The schedule of collection of fecal and blood samples is given in Figure 1A and included samples at day 0 (pre-treatment), two weeks, one month, two months, six months, and at treatment completion. TB bacterial load in sputum was measured at the same time points by recording time to culture positivity (TTP) in a BACTEC liquid culture system as a quantitative microbiologic measure of disease resolution (21). The antibiotic regimen used to treat these individuals included bedaquiline, linezolid, levofloxacin, clofazimine, and pyrazinamide for the first six months. All drugs were continued until treatment completion at 20–24 months except bedaquiline (stopped after six months) and linezolid (stopped after 12 months). See data file S1 for individual subject sampling and metadata.

Antibiotic treatment reduced *M. tuberculosis* (Mtb) bacterial load in sputum (corresponding to increased TTP) over time compared to baseline TTP ($p < 0.001$) for the linear mixed-effects model $TTP \sim Sex + Age + Time + 1|ID$ (Figure 1B). The rate of sputum sterilization was variable during early treatment, with some subjects achieving culture negativity (TTP > 1000) by one month of treatment and all achieving culture negativity by 6 months or treatment completion.

To investigate gastrointestinal microbiome changes that accompany MDR TB treatment, we determined the microbial composition and gene content using metagenomic sequencing of stool. We used Principal Coordinate Analysis on centered log-ratio transformed data(22) to account for compositionality in the abundance of both species and metabolic pathways. Our analysis revealed significant statistical differences between samples taken at baseline or treatment completion compared to earlier samples (2 weeks, 2 months, 6 months) for both species and functional pathway abundance based on repeated measures PERMANOVA (23) (p-value < 0.05, see data file S2). We observed that 23.6% of the variation in microbiome species abundance (Figure 1C) and 40.1% of the variation in pathway abundance (Figure 1D) encoded by Axis 1 could be attributed to treatment-induced changes in the microbiome occurring within the first six months compared to baseline and treatment completion (p-value < 0.05 based on linear mixed-effects modeling to predict the distribution of each individual principal coordinate axis as in (24). The second axis indicated variability in early MDR TB response (2 weeks, 1 month, and 2 months) among the different individuals.

To evaluate the effect of MDR TB treatment on microbiome alpha diversity while controlling for other variables, we regressed the Inverse Simpson Diversity Index (25) via linear mixed-effects modeling as $Diversity \sim Sex + Age + Time + 1|ID$. We observed a rapid loss of microbiome diversity within two weeks of treatment initiation that was sustained through 1-month, 2-month, and 6-month time points (p-value < 0.05 linear mixed-effects modeling) (Figure 1E). At the treatment completion visit, microbiome diversity had returned to baseline with variable recovery between subjects. Because the timing of sample collection at treatment completion was variable and did not coordinate exactly with antibiotic discontinuation (see table S1), we analyzed microbiome diversity at this timepoint as a function of the timing of antibiotic discontinuation and found no association (Figure 1E, inset) (P value > 0.05, linear regression modeling), indicating that the recovery of microbiome diversity could represent a form of adaptation to MDR TB treatment.

We then sought to identify microbial species and metabolic pathways affected by MDR TB treatment, both in comparison to pre-treatment and to our prior findings with treatment of drug-sensitive TB disease. On the taxonomic level, with the exception of the flavonoid-degrading Clostridia *Flavonifractor plautii* (26), the abundance of which increased with treatment, MDR TB treatment caused a depletion in the gastrointestinal microbiome during the first six months (Benjamini-Hochberg false discovery rate [FDR]<0.05). This coincided with a broad loss of species including *Bacteroides uniformis*, *Blautia spp.*, *Clostridium bolteae*, *Dorea longicatena, Eubacterium halli*, *Feacalibacterium prausnitzii*, *Phascolarctobacterium spp.*, and *Roseburia hominis*, known to be involved in the production of several bioactive metabolites such as short-chain fatty acids, succinate, and vitamins (27, 28), as well as bile acid transformation (29) (Figure 1F). Although this pattern resembles our prior findings in subjects treated for drug-sensitive TB with HRZE (21), the depletion encompasses more taxa in the MDR TB-treated individuals compared to HRZE. For example, a cluster of Clostridia that includes representatives of *Dorea*, *Eubacterium*, *Blautia*, and others was significantly more depressed by MDR TB treatment than by HRZE during early treatment (figure S1). In addition to broad commensal depletion, MDR TB treatment (but not HRZE) also caused an expansion of pathobionts including *Klebsiella*

pneumoniae, *Klebsiella varicola*, *Escherichia coli, Citrobacter werkmanii*, *Enterococcus avium,* and *Enterococcus faecium*(13) (FDR<0.05) (Figure 1F, fig. S1). These microbes are positively selected by antibiotic treatment because of higher antibiotic-induced redox potential, which includes increased gut epithelial oxygenation (30–32). For this reason, they are referred to as oxygen-tolerant pathobionts(13, 21). As observed for overall diversity, which rebounds to pretreatment levels late in the treatment course (Figure 1E), most of the species depleted by the antibiotics also returned to pre-treatment baseline by six months and were nearly completely restored by treatment cessation (Figure 1F), indicating unexpected microbiome resilience.

To determine whether the taxonomic perturbation was accompanied by alteration of the predicted functional coding capacity of the microbiome, we mapped metagenomic reads to the MetaCyc database using HUMAnN 3(33) and found that 33 metabolic pathways were depressed at any of the time points after MDR TB treatment compared to baseline (day 0) (Figure S2A). Consistent with the species-level analysis showing depression in known fiber-degrading and short-chain fatty acid-producing bacteria(34), MDR TB treatment also reduced the abundance of pathways involved in the degradation of fibers such as mannans and fructans as well as the *Bifidobacterium* shunt(35), leading to the formation of short-chain fatty acids (2-oxobutanoate degradation)(28). By contrast, between two weeks and six months of treatment, we found significant enrichment of several pathways previously associated with dysbiotic and inflammatory conditions (Figure S2B), including LPS biosynthesis and two known signatures of IBD (36, 37). We also observed greater enrichment of pathways indicating a relative expansion of facultative aerobic taxa (*Enterobacteriaceae* and Bacilli) (38) than seen with standard TB therapy (Figure S2C). In parallel with the restoration of species abundance (Figure 1F), the microbiome of MDR TB-treated individuals returned to a pre-treatment-like functional state by treatment cessation. Taken together, these data indicate that MDR treatment has an initial rapid effect on the taxonomic and functional output of the microbiome, with depletion of Clostridia and their associated pathways and enhancement of inflammatory pathobionts. Furthermore, we detect microbiome resilience marked by the restoration of pre-treatment composition and metabolic output at the end of therapy.

Inflammatory resolution of TB disease is a combined effect of pathogen killing and microbiome perturbation

Our prior work built computational models that quantitated the relative contributions of pathogen clearance and microbiome changes to the temporal resolution of the inflammatory state that accompanies TB, as measured by peripheral blood transcriptomics (21). These models deduced both pathogen-dependent and microbiome-dependent changes, with the dominant effect driven by antibiotic-driven pathogen reduction. We applied this approach to the longer treatment regimens of MDR TB and the severe microbiome disruption noted above. Consistent with the reduction in *M. tuberculosis* bacterial load with treatment, we observed a significant reduction in the expression of common inflammatory (IFN-α, IFN-γ, IL-6, JAK STAT3) and signaling pathways (TNFα γ, IL2, STAT5) during treatment (FDR < 0.05) (Figure S3A). Similarly, we observed a significant reduction in the expression of most

TB signatures particularly after six months of treatment and at treatment completion (FDR < 0.05) (Figure S3B).

We next sought to decouple the relative associations of microbiome perturbation and Mtb sterilization in the inflammatory resolution that accompanies TB treatment (Figure S3). Given the clear relationship between microbiome commensals and specific immune responses(39–43), we hypothesized that inter-individual variability in microbiome dynamics or bacterial load reduction (TTP) would be significantly associated with the inflammatory resolution that accompanies TB treatment. We applied mixed-effects random forest regression modeling to test this hypothesis. Briefly, for every MSigDB hallmark pathway or TB signature (see Figure S3) we fit the model $NES_{s,i} \sim f(TTP, X)_i + 1|ID$, where NES is the Normalized Enrichment Score for hallmark pathway (or signature) s in sample i, f is a general non-linear function (the random forest) applied to TTP and species relative abundances X in sample i as fixed effects, and $1|ID$ indicates the random effect to account for multiple samples from the same patient. To determine the significance of model-inferred associations, we used permutated importance analysis (44). For the significant associations obtained from the permutated importance calculations (FDR < 0.1), we then applied univariate linear mixed-effects models to determine the directionality (positive/negative) of the association. We deemed the use of this approach appropriate for analyzing the “large p, small n” multi-omics data that are commonly encountered in clinical research (45). Specifically, this machine learning method offers significant advantages over traditional multi-linear regression techniques as it is agnostic to model structure, enables non-parametric regression, and eliminates the need to fulfill assumptions underlying classical regression techniques. Additionally, this method inherently performs ranked feature selection. Although this may seem less direct compared to traditional regression, downstream analysis such as permutated importance(46) enables estimation of predictor significance on the dependent variable. Notably, for most of the hallmark pathways and TB signatures, reduction in Mtb bacterial load (TTP) was the most important predictor (Figure 2). Higher TTP (lower level of Mtb) associated with lower NES of several signatures related to inflammation (inflammatory response, interferon alpha, interferon gamma, and IL-6 JAK STAT3 signaling) and signaling (IL-2 STAT5 signaling, TNF-α signaling via NFKB, KRAS signaling) (Figure 2A), and almost all TB-associated gene signatures (Figure 2B). Several microbiome species also significantly associated with both hallmark pathway and TB signature enrichment scores. Specifically, a higher abundance of commensals that include short-chain fatty acid-producing Clostridia Cluster IV and XIVa (*Dorea longicatena*, *Erysipelatoclostridium ramosum*, *Gemmiger formicilis*, *Ruthenibacterium lactatiformans*) was associated with reduced peripheral inflammatory pathways and contributed to expression of most TB signatures. By contrast, a higher abundance of dysbiosis-associated oxygen-tolerant *Enterobacteriaceae* was associated with increased peripheral inflammation, immune signaling (Figure 2A), and enrichment of TB-associated gene signatures (Figure 2B). These observations independently validate recent findings with HRZE therapy (21) and suggest that the resolution of the transcriptomic markers of active TB disease during MTB treatment is associated with both pathogen sterilization and microbiome alterations. Taken together, our analysis suggests that a higher abundance of Clostridia clusters IV and XIVa(47) and lower levels of dysbiosis-associated *Enterobacteriaceae* are associated with

faster resolution of TB-associated peripheral inflammation. Importantly, compared to HRZE study in where we observe sterilization (as measured by changes in TTP) still occurring by 6 months of treatment, the MDR treatment data are characterized by a long period of antibiotic administration after TB culture negativity (6 months). By including 6-month to treatment completion timecourse data in our analysis we not only amplified the signal captured in (21) but were able to, more directly, infer microbiome's contribution to peripheral inflammation.

MDR TB treatment promotes antibiotic resistance in the microbiome

A large body of work has demonstrated that broad-spectrum antibiotics cause an increase in antibiotic-resistance genes in the gastrointestinal tract (48–51). We quantified the effect of TB treatment on the gut resistome in terms of duration, magnitude, and category of resistance. Shotgun metagenomic reads, for both the MDR TB treated cohort and our previously published longitudinal observational HRZE cohort (21), were mapped to a database of antibiotic resistance genes constructed from the 2021 Comprehensive Antibiotic Resistance Database (CARD version 3.13) as in(52). We found significant enrichment of ARGs in the microbiome by MDR TB treatment compared to baseline (day 0), an effect that encompassed broad antibiotic classes (Figure 3A). Two weeks of MDR TB treatment caused a significant enrichment (FDR < 0.05) in the abundance of 97 ARGs across the MDR TB-treated cohort (Figure 3B) encoding for resistance to major broad-spectrum antibiotic classes, with the highest representation of resistance to beta-lactams, fluoroquinolones, aminoglycosides, and macrolides (Figure 3C). Of these ARGs, 86 were still significantly enriched at both 1 and 2 months of treatment compared to pre-treatment, whereas 75 remained enriched at 6 months post-treatment initiation. As observed for bacterial species and functional pathways most of the differentially abundant ARGs returned to baseline late in treatment. Similarly to the species-level abundance analysis, which did not show any significant enrichment in oxygen-tolerant pathobionts in HRZE-treated individuals, ARG enrichment in the longitudinal observational HRZE treatment cohort was less pronounced compared to the MDR TB treatment cohort, with only three ARGs showing significantly different abundance at any treatment point compared to baseline (Figure S4).

Microbiome recovery during MDR TB treatment is characterized by commensal evolution

The accepted model of antibiotic impact on the microbiome is that, at least for short-term antibiotic treatment, the microbiome remains in a perturbed (or dysbiotic) state and slowly recovers after treatment cessation but may never return to its baseline state (7, 14, 32). In this study and our previous study of standard TB therapy, we observed microbiome resilience characterized by the return of members of the Clostridiales order that are phylogenetically related to those lost early during treatment (21). Although several of these repopulating commensals are assigned to the same species as their pre-treatment counterparts, we hypothesized that the returning commensal taxa may represent distinct strains. We therefore searched for fine genomic differences in metagenomes for each taxon in pre-treatment samples compared to different timepoints in the six-month longitudinal observational HRZE cohort (21) and the MDR TB treatment cohort described above using Metagenomic Intra-species Diversity Analysis (MIDAS) (53–55). After using MIDAS to align reads and detect SNPs in the core genome, we investigated the evolution of species for

each treatment condition by using random forest classification to identify genetic features that distinguish the pretreatment genomes from genomes at different times during treatment.

For the MDR TB cohort, we analyzed the metagenomes of *Klebsiella* and *E. coli* that dominate during early treatment and found pre- and on-treatment *Klebsiella* and *E. coli* are distinguishable by SNP analysis compared to baseline (Figure S5). The SNPs that distinguished the two *Klebsiella* populations were in genes encoding stress response factors, including multiple membrane transporters such as *lsrA*, *mntB*, and others. We also detected SNPs in the gene encoding DNA topoisomerase IV, the primary target of quinolones, administered in the MDR regiment as levofloxacin (Figure S5A). Dominating *E. coli* strains were defined by differences in allele frequencies for genes encoding for trimethylamine−N−oxide reductase 2 which has been implicated with lower sensitivity to quinolones and aminoglycosides, as well as *mdtB*, encoding a component of a multidrug efflux pump (Figure S5B)(56, 57). These results indicate that dominating pathobionts have resistance mutations to the administered antibiotics that arise in temporal sequence with their dominance of the microbiome.

We then performed a similar analysis for resilient commensals that returned after initial depletion (such as Clostridia). We found that *Blautia A wexlerae* and *Dorea longicatena B* displayed significantly higher SNP diversity at treatment completion compared to day 0 (Figure 4A,B). Principal component analysis of the allele frequencies for both microbes identified significant sample clustering based on sampling time (day 0 vs. treatment completion) (PERMANOVA < 0.05) (Figure 4C,D), suggesting strain replacement during microbiome recovery. For *Blautia*, the SNPs that distinguished pre-treatment from treatment completion included two proteins involved in DNA metabolism (DNA topoisomerase 3 and DNA helicase IV) and three proteins involved in translation (Figure 4E). In resilient *Dorea* strains, we detected mutations in multiple subunits of ATP synthases (Figure 4F). The F1F0 ATP synthase is the direct target of bedaquiline in mycobacteria(58) which binds the C ring (encoded by *atpE*), and mutations in *atpE* confer resistance to the drug (59). Overexpression of the ε subunit, in which we identifed mutations, can confer resistance to BDQ in *M. smegmatis*, although no resistance mutations have previously been identified in *M. tuberculosis in vitro* or in clinical isolates(60). We also detected mutations in related pathways of energy metabolism and glycerol kinase. Notably, both bedaquiline and clofazimine affect electron transport in mycobacteria and share multiple common resistance mutations, including glycerol kinase mutations *in vitro* (61), which has also been broadly linked to drug resistance(62, 63).

The presence of SNPs in ATP synthase and associated energy pathways in *Dorea* strongly suggests that this commensal may have evolved resistance, but bedaquiline and clofazimine have no known activity against commensal anaerobes. To determine whether bedaquiline and clofazimine have unanticipated activity on these commensals, we tested for activity against wildtype *D. longicatena* and *Blautia in vitro* (64) in anaerobic conditions. We found that bedaquiline inhibited two different *Blautia* species and *D. longicatena* beginning at 3 μg/ml, indicating a broad activity of bedaquiline against commensal anaerobes. Clofazimine similarly inhibited *Blautia* and *D. longicatena* between 1 and 10 μg/ml (Figure 4G). To determine whether clostridial inhibitory concentrations of these drugs were present in the

stool of treated patients, we measured concentrations of the administered drugs in stool samples taken at six months of treatment. We found a broad range of concentrations, likely due to variable time from drug dosing and sample collection, but with a mean concentration of bedaquiline of 30.5 μg/ml, near the inhibitory concentration measured *in vitro*. We also found average levofloxacin concentrations of 309.0 μg/ml (Figure 4H), well above the minimum inhibitory concentration (MIC) for gram-negative pathobionts (65) in which we observed resistance mutations. Clofazimine concentrations were ~100 μg/ml, well above the reported MIC for *Clostridioides difficile*(66) and 10–100 times above our measured MIC for *Blautia* and *Dorea*. These data indicate that commensal Clostridia are unexpectedly sensitive to bedaquiline and clofazimine at concentrations that occur in stool during therapy and that putative resistance mutations emerge coincident with commensal resilience.

The data above strongly suggest that the evolution of commensal resistance mutations to the administered anti-mycobacterial drugs is a mechanism of commensal resilience. To validate these findings, we next examined commensal evolution during standard TB therapy during which we previously observed clostridial resilience despite ongoing antibiotic administration (21). Random forest classification identified SNPs in *Phascolarctobacterium A succinatutens* and *Gemmiger formicilis* as two strong features differentiating pre-treatment and treatment completion samples. Quantitation of the abundance of these two taxa over the course of treatment revealed initial depletion followed by the return of abundance by 2 and 6 months (Figure 4I,J). The SNPs that most strongly distinguished initial from repopulating strains were in the *rpoB* encoded B subunit of RNA polymerase, the direct target of rifampicin and the site of rifampin resistance mutations (67)(Figure 4K,L). All six-month samples in which *Phascolarctobacterium A succinatutens* was detected had a SNP corresponding to position 450 in Mtb RpoB protein, including three with the S450Y substitution known to cause rifampin resistance (68–70) (Figure 4M). In *Gemminger formicilis*, all late treatment samples that demonstrated resilience contained the H445N substitution (Figure 4N), reported to confer rifampin resistance in Mtb, *Clostridioides difficile*, and *S. aureus* (68, 71, 72).

To determine whether the drug target mutations identified by MIDAS were widespread across the microbiome, we employed the inStrain (73) pipeline, which has greater sensitivity for single nucleotide variants. Our attention was directed towards the genetic loci that exhibited differentiation between the baseline and end-of-treatment samples in both the MDR TB treatment and the standard therapy (HRZE) cohorts. This analysis confirmed many of the MIDAS-detected variants, including in the ATP synthase epsilon chain and *glpK*, (Figure 5A-B and data file S3). Notably, inStrain also revealed mutations in the direct target of bedaquiline, the C subunit of ATP synthase encoded by *atpE*, in *S. salivarius* and *Prevotella* (Figure 5C). To determine the relationship of these *atpE* mutations to known BDQ resistance mutations, we performed structural modeling using the AlphaFold predicted structures of the C subunit, which revealed that the *S. salivarius* and *Prevotella* mutations are very close to the D28 and I66 sites in the *M. tuberculosis* protein which confer BDQ resistance when mutated (59) (Figure 5D). inStrain also identified non-synonymous mutations in *gyrA*, the target of fluoroquinolones (Figure 5E and data file S3). Mutations at alanine 90 of *M. tuberculosis* GyrA (74) confer quinolone resistance and structural modeling of three GyrA mutations from MDR treated subjects revealed exact overlap

with this hotspot (Figure 5F), strongly suggesting that these mutations confer quinolone resistance. Applying inStrain to HRZE treated microbiomes revealed the RpoB S450Y and H445N substitutions in *P. succinatutens* and *G. formicilis*, as initially identified by MIDAS, but also discovered numerous other mutations in additional taxa at these positions in RpoB, as well as at additional positions in RpoB known to confer rifampin resistance (75) (Figure 5G and data file S3). These data provide strong evidence that resistance mutations to the administered antibiotics evolve widely in commensals and are temporally correlated with commensal resilience to ongoing antibiotics. Altogether, this analysis indicates that selection of antimicrobial-resistant commensals and pathobionts may impact microbiome dynamics during long-term antibiotic therapy and that, ultimately, microbiome resilience may be due to out-competition of resistant pathobionts by more fit and drug-resistant commensals.

Functional microbiome resilience to bedaquiline *in vivo*

To directly demonstrate whether the resilient microbiome was indeed functionally resistant to antibiotic disruption, we colonized mice by fecal matter transplant (FMT) with pooled stool from three individuals who completed MDR TB treatment (TC) or pooled from three healthy community controls (HC)(21). After FMT, mice were treated with one week of bedaquiline or vehicle as in (76, 77) (Figure 6A). We first examined the mouse microbiome immediately after ampicillin, vancomycin, neomycin, and metronidazole (AVNM) treatment and found no difference between mice scheduled to receive TC vs. HC FMT, apart from each being enriched in a different *Streptococcus* phylotype (Figure S6A, B). Although we observed poor efficiency of engraftment of Clostridia into mice, *F. plautii*, the only Clostridia to be enriched by early MDR treatment in human samples, displayed the same behavior in TC-engrafted, but not HC-engrafted mice, and was the only species characterized by a significant increase (FDR < 0.05) in relative abundance (Figure S7 A,B). When examining the microbiome post-FMT and before bedaquiline/vehicle treatment, we found 58 species (FDR < 0.05) differentially abundant in TC- vs. HC-engrafted mice. Most of these differential species belonged to the genera *Bacteroides* and *Parabacteroides*, with some enriched in the TC samples and others in the HC samples (Figure S6C, D). To quantitate the effect of bedaquiline on TC vs. HC microbiome, we used Principle Component Analysis on the Bray-Curtis distance computed for every pair of samples during bedaquiline and vehicle treatment. Bedaquiline treated animals that received TC FMT exhibited closer proximity to their respective pre-treatment FMT animals compared to mice receiving HC FMT (Figure 6B). We then modeled the Bray-Curtis distance between (1) every vehicle sample to every other vehicle sample, (2) every vehicle sample to every bedaquiline sample, and (3) every bedaquiline sample to every other bedaquiline sample independently, as a function of treatment time, FMT type (HC/TC), and the interaction between the two using linear mixed-effects models. The mouse identifier was included as random effect. We chose this modeling approach because the degree of significance of the coefficients associated with the interaction terms allows quantitation of the likelihood that the type of donor stool affects the microbiome composition during treatment. We hypothesized that for the mice receiving vehicle, the distance to other vehicle recipients would not be affected by the microbiome used for FMT (TC vs. HC). By contrast, we expected that the microbiome of mice treated with bedaquiline would diverge from that of mice receiving vehicle if colonized with an HC but not a TC microbiome. Confirming

our hypothesis, whereas the distance among samples from mice receiving vehicle slightly increased with treatment duration, this change was independent of the stool source of FMT (p-value > 0.05) (Figure 6C). By contrast, comparisons between bedaquiline-treated groups or between vehicle- and bedaquiline-treated groups revealed an effect of treatment duration which strongly reflected the stool source of FMT (healthy (HC) vs. MDR TB treated (TC)) (FDR < 0.05, Figure 6D, E). The microbiome of HC recipient mice was strongly affected by bedaquiline treatment (regression line with significant positive slope) whereas mice that received TC FMT were unaffected (regression line substantially horizontal). These results demonstrate that the microbiome from MDR-treated human subjects is functionally resilient to antibiotic-induced disruption.

Discussion

Treatment of *M. tuberculosis* infection represents one of the longest continuous antibiotic exposures of humans. Recent work with individuals undergoing 6-month treatment for drug-sensitive Mtb demonstrated that renormalization of disease markers during treatment could be predicted by a combined model that incorporates pathogen sterilization and the extent of treatment-induced microbiome perturbation (21). These findings linked the well-documented perturbing effect of antibiotics on the human microbiome (6, 78) with their direct effects on host immunity (79) in human disease. In this work, we investigated MDR TB treatment, which is a significantly longer antibiotic course with both mycobacterial-specific and broad-spectrum agents. Our findings confirm, in an independent cohort with a distinct TB treatment regimen, that the resolution of TB inflammatory disease markers is a combined effect of pathogen sterilization and microbiome alteration. Thus microbiome composition has a substantial effect in shaping the dynamic tone of systemic inflammation, both in disease states and in homeostatic conditions. Our findings are consistent with prior findings in both humans and animals that Clostridia participate in the induction of anti-inflammatory states (80, 81), whereas blooms of *Enterobacteriaceae* contribute to inflammatory exacerbation (82). In addition to these insights into TB disease resolution, analysis of this prolonged antibiotic exposure provided unexpected insights into commensal contribution to long-term microbiome dynamics under continuous antibiotic pressure.

Accumulation and spread of multi-drug resistant organisms, particularly MDR *E. coli* and *Klebsiella*, is a major public health problem in both the healthcare and the community settings (83). Recent work has identified strong associations between the carriage of ARGs and the risk of developing of neonatal sepsis and adverse birth outcomes (84). Similarly, a higher abundance of ARGs and the associated organisms predict the occurrence of bloodstream infections in hematopoietic stem-cell transplantation patients (85). We find that MDR TB treatment causes a temporary (~six months) bloom of dysbiosis-associated oxygen-tolerant pathobionts such as *Enterobacteriaceae* and *Bacilli*. This bloom is characteristic of treatment of other broad-spectrum antibiotics (32), as well as what we observed after two weeks of treatment with the antiparasitic drug nitazoxanide in a clinical trial for the treatment of TB (21). These data also indicate that MDR TB treatment, but not standard TB treatment, enhances the AMR coding capacity of the microbiome across all antibiotic classes, including beta-lactams, fluoroquinolones, and macrolides. Importantly, although the abundance of these ARGs approaches pre-treatment baseline

by treatment cessation, the AMR expansion is persistent for at least the first six months of MDR TB treatment. Although there are scattered case reports of resistant infections in patients with MDR TB (86, 87), our data suggest that MDR TB treatment might be a risk factor for antimicrobial-resistant gram-negative infection. Such associations should be sought in future studies, both in individuals and in communities with high rates of MDR TB (88). Although we did not find AMR enhancement with HRZE therapy of drug-sensitive TB, recent data has validated four-month therapy for drug-sensitive TB that includes the quinolone moxifloxacin (89). Our data predicts that the microbiome effects of this quinolone-containing regimen might resemble MDR treatment, potentially broadening the threat of drug-resistant infections in TB-treated subjects, a possibility that should be considered as new TB regimens are tested.

Little is known about the degree by which intra-host microbiome evolution shapes host-microbiome temporal dynamics (90). Our findings document an unexpected resilience of the microbiome to disruption by long-term antibiotics and imply a mechanism by which the microbiome maintains homeostasis in the face of perturbation. We hypothesized that a possible resilience mechanism was microbiome adaptation to the treatment-induced environment, as has been hypothesized in theoretical work (91, 92). After an initial period of compositional imbalance with pathobiont domination, the microbiome spontaneously adapts with the re-establishment of commensal domination. Our data indicate that the mechanism of this resilience is the evolution of antimicrobial resistance mutations in the genomes of both pathobionts and commensals. The re-establishment of commensal domination, despite resistance mutations in both pathobionts and commensals, suggests that commensal fitness is superior if antimicrobial resistance emerges. Another question raised by our findings is the duration of commensal compensatory mutations within the microbiome. Although we might expect that these mutations would wane with increasing time off antibiotics, we note that the putative bedaquiline resistance mutations detected, and the bedaquiline resilience we demonstrate in mice, is present more than a year after discontinuation of the drug, suggesting that these mutations may have a fitness benefit in the microbiome ecosystem established by long-term antibiotics.

Our findings imply that the adverse consequences of antimicrobials on the microbiome, including the proliferation of ARGs, could be mitigated by enabling commensals to resist the effects of antimicrobials. Although it is difficult to determine causality in an observational human study, especially with the temporal changes in antibiotic pressure that occur in this study, our data nevertheless imply that commensals have an intrinsic capacity to outcompete pathobionts and the ARGs they encode if able to evolve under the selective pressures of antibiotics. Microbiome therapeutics, including fecal transplant, rational microbial consortia, and engineered probiotics are being pursued as a decolonization strategy for AMR-encoding pathobionts (93–95). Our data may suggest that antibiotic-tolerant commensal strains, possibly through resistance mutations, may paradoxically provide long-lasting suppression of AMR in the face of ongoing antibiotics and allow ongoing antibiotic therapy without the ordinarily deleterious effects on microbiome composition. Of course, one potential adverse consequence of resistant commensals is the proliferation of AMR. Still, this risk may depend on the transferability of the resistance element and the pathogenic potential of the commensal in question. Our study provides

a paradigm by which commensal resilience to antibiotics can be potentially leveraged to paradoxically counter AMR.

The nature of this observational human study prevents us from definitively concluding that the recovery in microbiome composition (including species, pathways, and ARG abundances) is solely attributed to the observed mutations in commensals. To make such a determination, it would be necessary to isolate the resistant commensals and conduct further testing for resistance and fecal microbiota transplantation. However, we did demonstrate that stool samples from individuals undergoing MDR treatment, when transplanted into mice, retained resistance to bedaquiline. Additionally, the data from the HRZE cohort revealed the emergence of mutations known to confer resistance to rifampin, providing direct evidence that these drugs act as a selective pressure influencing the evolutionary dynamics of the microbiome.

Materials and Methods

Study design

The targeted enrollment was 60 subjects. 31 subjects signed consent and 24 subjects passed enrollment screening. The study was powered for the primary endpoints which were detection of DD-MTB in sputum and a 20 gene transcriptomic signature, neither of which is included in this report. The microbiome analysis was a prespecified secondary endpoint but did not contribute to the power calculation. All data collection time points and sample types were prespecified in the protocol and were not altered by intermediate analyses. No data was excluded, and any missing data points are due to nonavailability of samples due to sample or patient dropout. No outlier definitions were used, and outliers were not excluded from any data analysis.

The primary and secondary endpoints were prospectively specified in the clinical protocol with the microbiome analyses as a secondary endpoint.

For each clinical time point, only one sample was available (stool, blood, sputum). For microbiome DNA and peripheral blood RNA, one sample was prepared and sequenced as specified. For sputum TTP determination, duplicate measurements on a single sputum sample were performed at the TTP was an average of the two values, except due to technical dropout, as specified in the supplementary data.

All volunteers provided written informed consent to participate in this study. All human studies were reviewed and approved by the IRBs of both Weill Cornell Medicine and Groupe Haitien d’etude du Sarcome de Kaposi et des Infections Opportunistes (GHESKIO) Centers (Port-au-Prince, Haiti). Participants provided informed consent prior to peripheral blood draw for whole blood collection and stool collection for metagenomic sequencing. All methods and procedures were performed in accordance with the relevant institutional guidelines and regulations. Mouse studies were approved by the UMass Chan Institutional Animal Care and Use Committee under protocol PROTO202100184. Specifically, housing conditions for experimental animals were maintained in individual cages equipped with appropriate bedding and environmental enrichment. A 12-hour light-

dark cycle was regulated to simulate natural conditions, and a standardized feeding regimen was implemented to ensure consistency across all subjects. Each cage housed a single animal to minimize potential confounding variables.

MDR TB treatment longitudinal cohort

The purpose of this study was to determine 1) the effect of antibiotics used for the treatment of MDR TB on the composition of stool microbiome and 2) use longitudinal data of MDR treatment, including microbiome composition and peripheral blood transcriptomics to model the resolution of TB disease. This study was a single arm observational, non-randomized and non-blinded study of subjects with MDR TB undergoing treatment with a standard regimen (defined above). Donors were enrolled through the Clinical Trials Unit at GHESKIO. Pulmonary TB was diagnosed by clinical symptoms, chest radiograph consistent with pulmonary TB, and positive molecular testing. No other formal enrollment criteria were required, such as prior antibiotic treatment. All participant samples were deidentified on-site using a barcode system before they were shipped to Weill Cornell Medicine (WCM)/ Memorial Sloan Kettering Cancer Center (MSKCC) for analysis. All clinical metadata was collected on-site and managed through the REDCap data management system (101).

Statistical analysis

Linear mixed-effects models were run to identify significant associations between sex, age, and treatment duration on microbiome diversity on time to positivity and microbiome diversity. Significance was determined at FDR < 0.05. Repeated measurement PERMANOVA was run to quantify variance and test for compositional differences explained by experimental and subject features in every principal coordinate analysis in the microbiome data. Linear mixed-effects models were run to identify microbial species, pathways, ARGs and host genes associated with sex, age, and treatment duration. Significance was determined at FDR < 0.05. For the *in vitro* antibiotic susceptibility experiments, ANOVA followed by Tukey-post hoc tests were used to determine significant differences in OD due to different treatment concentrations. Linear mixed-effects modeling was used to assess FMT-dependent effects on how the microbiome evolves in response to bedaquiline/vehicle treatment in the *in vivo* microbiome reconstitution experiments. Significance was determined at P < 0.05. Mixed-effects Random Forest (MERF) regression modeling was used to assess the relative contribution of the gastrointestinal microbiome and *Mtb* dynamics towards peripheral gene expression. Significance of the model-inferred associations we used permutated importance analysis at an FDR < 0.1. Further details are available in the supplementary materials.

Supplementary Material

Refer to Web version on PubMed Central for supplementary material.

Acknowledgments:

We thank Cindy Lai for assistance with manuscript preparation and editing, and Alexander Rudensky for feedback.

Funding:

This study was funded by Tri-Institutional TB Research Unit (Tri-I TBRU) grant U19AI162568 (MSG, VB), Congressionally Directed Medical Research Programs (CDRMP) grant PRMP, W81XWH2020013 (VB), and Bill & Melinda Gates Foundation (VB). This research was funded in part through the NIH/NCI Cancer Center Support Grant P30 CA008748. Support for ChimeraX is supported by National Institutes of Health R01-GM129325 and the Office of Cyber Infrastructure and Computational Biology, National Institute of Allergy and Infectious Diseases.

References and Notes:

1. Langdon A, Crook N, Dantas G. The effects of antibiotics on the microbiome throughout development and alternative approaches for therapeutic modulation. Genome Med. 2016;8(1):39. Epub 2016/04/15. doi: 10.1186/s13073-016-0294-z. [PubMed: 27074706]
2. Reyman M, van Houten MA, Watson RL, Chu MLJN, Arp K, de Waal WJ, Schiering I, Plötz FB, Willems RJL, van Schaik W, Sanders EAM, Bogaert D. Effects of early-life antibiotics on the developing infant gut microbiome and resistome: a randomized trial. Nature Communications. 2022;13(1):893. doi: 10.1038/s41467-022-28525-z.
3. Fishbein SRS, Mahmud B, Dantas G. Antibiotic perturbations to the gut microbiome. Nature Reviews Microbiology. 2023. doi: 10.1038/s41579-023-00933-y.
4. Becattini S, Taur Y, Pamer EG. Antibiotic-Induced Changes in the Intestinal Microbiota and Disease. Trends Mol Med. 2016;22(6):458–78. Epub 2016/05/15. doi: 10.1016/j.molmed.2016.04.003. [PubMed: 27178527]
5. Dethlefsen L, Huse S, Sogin ML, Relman DA. The pervasive effects of an antibiotic on the human gut microbiota, as revealed by deep 16S rRNA sequencing. PLoS Biol. 2008;6(11):e280. Epub 2008/11/21. doi: 10.1371/journal.pbio.0060280. [PubMed: 19018661]
6. Dethlefsen L, Relman DA. Incomplete recovery and individualized responses of the human distal gut microbiota to repeated antibiotic perturbation. Proc Natl Acad Sci U S A. 2011;108 Suppl 1:4554–61. doi: 10.1073/pnas.1000087107. [PubMed: 20847294]
7. Bucci V, Bradde S, Biroli G, Xavier JB. Social interaction, noise and antibiotic-mediated switches in the intestinal microbiota. PLoS computational biology. 2012;8(4):e1002497. [PubMed: 22577356]
8. McFarland LV. Antibiotic-associated diarrhea: epidemiology, trends and treatment. Future Microbiol. 2008;3(5):563–78. Epub 2008/09/25. doi: 10.2217/17460913.3.5.563. [PubMed: 18811240]
9. Buffie CG, Bucci V, Stein RR, McKenney PT, Ling L, Gobourne A, No D, Liu H, Kinnebrew M, Viale A, Littmann E, van den Brink MRM, Jenq RR, Taur Y, Sander C, Cross JR, Toussaint NC, Xavier JB, Pamer EG. Precision microbiome reconstitution restores bile acid mediated resistance to Clostridium difficile. Nature. 2015;517(7533):205–8. doi: 10.1038/nature13828. [PubMed: 25337874]
10. Taur Y, Xavier JB, Lipuma L, Ubeda C, Goldberg J, Gobourne A, Lee YJ, Dubin KA, Socci ND, Viale A, Perales M-A, Jenq RR, van den Brink MRM, Pamer EG. Intestinal Domination and the Risk of Bacteremia in Patients Undergoing Allogeneic Hematopoietic Stem Cell Transplantation. Clinical Infectious Diseases. 2012;55(7):905–14. doi: 10.1093/cid/cis580. [PubMed: 22718773]
11. Schwartz DJ, Langdon AE, Dantas G. Understanding the impact of antibiotic perturbation on the human microbiome. Genome Medicine. 2020;12(1):82. doi: 10.1186/s13073-020-00782-x. [PubMed: 32988391]
12. Mao-Jones J, Ritchie KB, Jones LE, Ellner SP. How Microbial Community Composition Regulates Coral Disease Development. PLOS Biology. 2010;8(3):e1000345. doi: 10.1371/journal.pbio.1000345. [PubMed: 20361023]
13. Kim S, Covington A, Pamer EG. The intestinal microbiota: Antibiotics, colonization resistance, and enteric pathogens. Immunological Reviews. 2017;279(1):90–105. doi: 10.1111/imr.12563. [PubMed: 28856737]
14. Ng KM, Aranda-Díaz A, Tropini C, Frankel MR, Van Treuren W, O'Loughlin CT, Merrill BD, Yu FB, Pruss KM, Oliveira RA, Higginbottom SK, Neff NF, Fischbach MA, Xavier KB, Sonnenburg JL, Huang KC. Recovery of the Gut Microbiota after Antibiotics Depends on Host Diet, Community Context, and Environmental Reservoirs. Cell Host & Microbe. 2019;26(5):650–65.e4. doi: 10.1016/j.chom.2019.10.011. [PubMed: 31726029]

15. Roodgar M, Good BH, Garud NR, Martis S, Avula M, Zhou W, Lancaster SM, Lee H, Babveyh A, Nesamoney S, Pollard KS, Snyder MP. Longitudinal linked-read sequencing reveals ecological and evolutionary responses of a human gut microbiome during antibiotic treatment. Genome Research. 2021;31(8):1433–46. doi: 10.1101/gr.265058.120. [PubMed: 34301627]

16. Zhao S, Lieberman TD, Poyet M, Kauffman KM, Gibbons SM, Groussin M, Xavier RJ, Alm EJ. Adaptive Evolution within Gut Microbiomes of Healthy People. Cell Host & Microbe. 2019;25(5):656–67.e8. doi: 10.1016/j.chom.2019.03.007. [PubMed: 31028005]

17. Garud NR, Good BH, Hallatschek O, Pollard KS. Evolutionary dynamics of bacteria in the gut microbiome within and across hosts. PLoS Biol. 2019;17(1):e3000102. Epub 2019/01/24. doi: 10.1371/journal.pbio.3000102. [PubMed: 30673701]

18. Tao C, Zhang Q, Zeng W, Liu G, Shao H. The effect of antibiotic cocktails on host immune status is dynamic and does not always correspond to changes in gut microbiota. Appl Microbiol Biotechnol. 2020;104(11):4995–5009. Epub 2020/04/19. doi: 10.1007/s00253-020-10611-1. [PubMed: 32303819]

19. Seung KJ, Keshavjee S, Rich ML. Multidrug-Resistant Tuberculosis and Extensively Drug-Resistant Tuberculosis. Cold Spring Harb Perspect Med. 2015;5(9):a017863. Epub 2015/04/29. doi: 10.1101/cshperspect.a017863. [PubMed: 25918181]

20. Pontali E, Raviglione MC, Migliori GB. Regimens to treat multidrug-resistant tuberculosis: past, present and future perspectives. European Respiratory Review. 2019;28(152):190035. doi: 10.1183/16000617.0035-2019. [PubMed: 31142549]

21. Wipperman MF, Bhattarai SK, Vorkas CK, Maringati VS, Taur Y, Mathurin L, McAulay K, Vilbrun SC, Francois D, Bean J, Walsh KF, Nathan C, Fitzgerald DW, Glickman MS, Bucci V. Gastrointestinal microbiota composition predicts peripheral inflammatory state during treatment of human tuberculosis. Nat Commun. 2021;12(1):1141. Epub 2021/02/20. doi: 10.1038/s41467-021-21475-y. [PubMed: 33602926]

22. Quinn TP, Erb I, Gloor G, Notredame C, Richardson MF, Crowley TM. A field guide for the compositional analysis of any-omics data. Gigascience. 2019;8(9). Epub 2019/09/24. doi: 10.1093/gigascience/giz107.

23. Lloyd-Price J, Arze C, Ananthakrishnan AN, Schirmer M, Avila-Pacheco J, Poon TW, Andrews E, Ajami NJ, Bonham KS, Brislawn CJ, Casero D, Courtney H, Gonzalez A, Graeber TG, Hall AB, Lake K, Landers CJ, Mallick H, Plichta DR, Prasad M, Rahnavard G, Sauk J, Shungin D, Vázquez-Baeza Y, White RA, Bishai J, Bullock K, Deik A, Dennis C, Kaplan JL, Khalili H, McIver LJ, Moran CJ, Nguyen L, Pierce KA, Schwager R, Sirota-Madi A, Stevens BW, Tan W, ten Hoeve JJ, Weingart G, Wilson RG, Yajnik V, Braun J, Denson LA, Jansson JK, Knight R, Kugathasan S, McGovern DPB, Petrosino JF, Stappenbeck TS, Winter HS, Clish CB, Franzosa EA, Vlamakis H, Xavier RJ, Huttenhower C, Investigators I. Multi-omics of the gut microbial ecosystem in inflammatory bowel diseases. Nature. 2019;569(7758):655–62. doi: 10.1038/s41586-019-1237-9. [PubMed: 31142855]

24. Olm MR, Dahan D, Carter MM, Merrill BD, Yu FB, Jain S, Meng X, Tripathi S, Wastyk H, Neff N, Holmes S, Sonnenburg ED, Jha AR, Sonnenburg JL. Robust variation in infant gut microbiome assembly across a spectrum of lifestyles. Science. 2022;376(6598):1220–3. doi: 10.1126/science.abj2972. [PubMed: 35679413]

25. Wagner BD, Grunwald GK, Zerbe GO, Mikulich-Gilbertson SK, Robertson CE, Zemanick ET, Harris JK. On the Use of Diversity Measures in Longitudinal Sequencing Studies of Microbial Communities. Frontiers in Microbiology. 2018;9(1037). doi: 10.3389/fmicb.2018.01037.

26. Mikami A, Ogita T, Namai F, Shigemori S, Sato T, Shimosato T. Oral Administration of Flavonifractor plautii, a Bacteria Increased With Green Tea Consumption, Promotes Recovery From Acute Colitis in Mice via Suppression of IL-17. Frontiers in Nutrition. 2021;7. doi: 10.3389/fnut.2020.610946.

27. Parada Venegas D, De la Fuente MK, Landskron G, González MJ, Quera R, Dijkstra G, Harmsen HJM, Faber KN, Hermoso MA. Short Chain Fatty Acids (SCFAs)-Mediated Gut Epithelial and Immune Regulation and Its Relevance for Inflammatory Bowel Diseases. Frontiers in Immunology. 2019;10(277). doi: 10.3389/fimmu.2019.00277.

28. Louis P, Flint HJ. Formation of propionate and butyrate by the human colonic microbiota. Environmental Microbiology. 2017;19(1):29–41. doi: 10.1111/1462-2920.13589. [PubMed: 27928878]
29. Heinken A, Ravcheev DA, Baldini F, Heirendt L, Fleming RMT, Thiele I. Systematic assessment of secondary bile acid metabolism in gut microbes reveals distinct metabolic capabilities in inflammatory bowel disease. Microbiome. 2019;7(1):75. doi: 10.1186/s40168-019-0689-3. [PubMed: 31092280]
30. Rivera-Chávez F, Zhang LF, Faber F, Lopez CA, Byndloss MX, Olsan EE, Xu G, Velazquez EM, Lebrilla CB, Winter SE, Bäumler AJ. Depletion of Butyrate-Producing Clostridia from the Gut Microbiota Drives an Aerobic Luminal Expansion of Salmonella. Cell Host Microbe. 2016;19(4):443–54. Epub 2016/04/15. doi: 10.1016/j.chom.2016.03.004. [PubMed: 27078066]
31. Kelly CJ, Zheng L, Campbell EL, Saeedi B, Scholz CC, Bayless AJ, Wilson KE, Glover LE, Kominsky DJ, Magnuson A, Weir TL, Ehrentraut SF, Pickel C, Kuhn KA, Lanis JM, Nguyen V, Taylor CT, Colgan SP. Crosstalk between Microbiota-Derived Short-Chain Fatty Acids and Intestinal Epithelial HIF Augments Tissue Barrier Function. Cell Host Microbe. 2015;17(5):662–71. Epub 2015/04/14. doi: 10.1016/j.chom.2015.03.005. [PubMed: 25865369]
32. Reese AT, Cho EH, Klitzman B, Nichols SP, Wisniewski NA, Villa MM, Durand HK, Jiang S, Midani FS, Nimmagadda SN. Antibiotic-induced changes in the microbiota disrupt redox dynamics in the gut. Elife. 2018;7:e35987. [PubMed: 29916366]
33. Beghini F, McIver LJ, Blanco-Míguez A, Dubois L, Asnicar F, Maharjan S, Mailyan A, Manghi P, Scholz M, Thomas AM, Valles-Colomer M, Weingart G, Zhang Y, Zolfo M, Huttenhower C, Franzosa EA, Segata N. Integrating taxonomic, functional, and strain-level profiling of diverse microbial communities with bioBakery 3. eLife. 2021;10:e65088. doi: 10.7554/eLife.65088. [PubMed: 33944776]
34. Olendzki B, Bucci V, Cawley C, Maserati R, McManus M, Olednzki E, Madziar C, Chiang D, Ward DV, Pellish R, Foley C, Bhattarai S, McCormick BA, Maldonado-Contreras A. Dietary manipulation of the gut microbiome in inflammatory bowel disease patients: Pilot study. Gut Microbes. 2022;14(1):2046244. Epub 2022/03/22. doi: 10.1080/19490976.2022.2046244. [PubMed: 35311458]
35. Ma W, Nguyen LH, Song M, Wang DD, Franzosa EA, Cao Y, Joshi A, Drew DA, Mehta R, Ivey KL, Strate LL, Giovannucci EL, Izard J, Garrett W, Rimm EB, Huttenhower C, Chan AT. Dietary fiber intake, the gut microbiome, and chronic systemic inflammation in a cohort of adult men. Genome Medicine. 2021;13(1):102. doi: 10.1186/s13073-021-00921-y. [PubMed: 34140026]
36. Amos GCA, Sergaki C, Logan A, Iriarte R, Bannaga A, Chandrapalan S, Wellington EMH, Rijpkema S, Arasaradnam RP. Exploring how microbiome signatures change across inflammatory bowel disease conditions and disease locations. Scientific Reports. 2021;11(1):18699. doi: 10.1038/s41598-021-96942-z. [PubMed: 34548500]
37. Park SK, Kim HN, Choi CH, Im JP, Cha JM, Eun CS, Kim TO, Kang SB, Bang KB, Kim HG, Jung Y, Yoon H, Han DS, Lee CW, Ahn K, Kim HL, Park DI. Differentially Abundant Bacterial Taxa Associated with Prognostic Variables of Crohn's Disease: Results from the IMPACT Study. J Clin Med. 2020;9(6). Epub 2020/06/11. doi: 10.3390/jcm9061748.
38. Hughes ER, Winter MG, Duerkop BA, Spiga L, Furtado de Carvalho T, Zhu W, Gillis CC, Büttner L, Smoot MP, Behrendt CL, Cherry S, Santos RL, Hooper LV, Winter SE. Microbial Respiration and Formate Oxidation as Metabolic Signatures of Inflammation-Associated Dysbiosis. Cell Host Microbe. 2017;21(2):208–19. Epub 2017/02/10. doi: 10.1016/j.chom.2017.01.005. [PubMed: 28182951]
39. Atarashi K, Tanoue T, Oshima K, Suda W, Nagano Y, Nishikawa H, Fukuda S, Saito T, Narushima S, Hase K, Kim S, Fritz JV, Wilmes P, Ueha S, Matsushima K, Ohno H, Olle B, Sakaguchi S, Taniguchi T, Morita H, Hattori M, Honda K. Treg induction by a rationally selected mixture of Clostridia strains from the human microbiota. Nature. 2013;500(7461):232–6. Epub 2013/07/12. doi: 10.1038/nature12331. [PubMed: 23842501]
40. Arpaia N, Campbell C, Fan X, Dikiy S, van der Veeken J, deRoos P, Liu H, Cross JR, Pfeffer K, Coffer PJ, Rudensky AY. Metabolites produced by commensal bacteria promote peripheral regulatory T-cell generation. Nature. 2013;504(7480):451–5. doi: 10.1038/nature12726. [PubMed: 24226773]

41. Atarashi K, Tanoue T, Shima T, Imaoka A, Kuwahara T, Momose Y, Cheng G, Yamasaki S, Saito T, Ohba Y, Taniguchi T, Takeda K, Hori S, Ivanov II, Umesaki Y, Itoh K, Honda K. Induction of colonic regulatory T cells by indigenous Clostridium species. Science. 2011;331(6015):337–41. doi: 10.1126/science.1198469. [PubMed: 21205640]
42. Ivanov II, Atarashi K, Manel N, Brodie EL, Shima T, Karaoz U, Wei D, Goldfarb KC, Santee CA, Lynch SV, Tanoue T, Imaoka A, Itoh K, Takeda K, Umesaki Y, Honda K, Littman DR. Induction of intestinal Th17 cells by segmented filamentous bacteria. Cell. 2009;139(3):485–98. Epub 2009/10/20. doi: 10.1016/j.cell.2009.09.033. [PubMed: 19836068]
43. Tanoue T, Morita S, Plichta DR, Skelly AN, Suda W, Sugiura Y, Narushima S, Vlamakis H, Motoo I, Sugita K, Shiota A, Takeshita K, Yasuma-Mitobe K, Riethmacher D, Kaisho T, Norman JM, Mucida D, Suematsu M, Yaguchi T, Bucci V, Inoue T, Kawakami Y, Olle B, Roberts B, Hattori M, Xavier RJ, Atarashi K, Honda K. A defined commensal consortium elicits CD8 T cells and anti-cancer immunity. Nature. 2019;565(7741):600–5. Epub 2019/01/25. doi: 10.1038/s41586-019-0878-z. [PubMed: 30675064]
44. Haran JP, Ward DV, Bhattarai SK, Loew E, Dutta P, Higgins A, McCormick BA, Bucci V. The high prevalence of Clostridioides difficile among nursing home elders associates with a dysbiotic microbiome. Gut Microbes. 2021;13(1):1–15. Epub 2021/03/26. doi: 10.1080/19490976.2021.1897209.
45. Johnstone IM, Titterington DM. Statistical challenges of high-dimensional data. Philos Trans A Math Phys Eng Sci. 2009;367(1906):4237–53. Epub 2009/10/07. doi: 10.1098/rsta.2009.0159. [PubMed: 19805443]
46. Altmann A, Tolosi L, Sander O, Lengauer T. Permutation importance: a corrected feature importance measure. Bioinformatics. 2010;26(10):1340–7. Epub 2010/04/14. doi: 10.1093/bioinformatics/btq134. [PubMed: 20385727]
47. Lopetuso LR, Scaldaferri F, Petito V, Gasbarrini A. Commensal Clostridia: leading players in the maintenance of gut homeostasis. Gut Pathog. 2013;5(1):23. Epub 2013/08/15. doi: 10.1186/1757-4749-5-23. [PubMed: 23941657]
48. Francino M. Antibiotics and the human gut microbiome: dysbioses and accumulation of resistances. Frontiers in microbiology. 2016:1543. [PubMed: 26793178]
49. Anthony WE, Wang B, Sukhum KV, D'Souza AW, Hink T, Cass C, Seiler S, Reske KA, Coon C, Dubberke ER, Burnham C- AD, Dantas G, Kwon JH. Acute and persistent effects of commonly used antibiotics on the gut microbiome and resistome in healthy adults. Cell Reports. 2022;39(2):110649. doi: 10.1016/j.celrep.2022.110649. [PubMed: 35417701]
50. Willmann M, Vehreschild MJGT, Biehl LM, Vogel W, Dörfel D, Hamprecht A, Seifert H, Autenrieth IB, Peter S. Distinct impact of antibiotics on the gut microbiome and resistome: a longitudinal multicenter cohort study. BMC Biology. 2019;17(1):76. doi: 10.1186/s12915-019-0692-y. [PubMed: 31533707]
51. Isles NS, Mu A, Kwong JC, Howden BP, Stinear TP. Gut microbiome signatures and host colonization with multidrug-resistant bacteria. Trends in Microbiology. 2022;30(9):853–65. doi: 10.1016/j.tim.2022.01.013. [PubMed: 35184972]
52. Ben Maamar S, Glawe AJ, Brown TK, Hellgeth N, Hu J, Wang JP, Huttenhower C, Hartmann EM. Mobilizable antibiotic resistance genes are present in dust microbial communities. PLoS Pathog. 2020;16(1):e1008211. Epub 2020/01/24. doi: 10.1371/journal.ppat.1008211. [PubMed: 31971995]
53. Nayfach S, Rodriguez-Mueller B, Garud N, Pollard KS. An integrated metagenomics pipeline for strain profiling reveals novel patterns of bacterial transmission and biogeography. Genome Res. 2016;26(11):1612–25. Epub 2016/11/03. doi: 10.1101/gr.201863.115. [PubMed: 27803195]
54. Zhao C, Dimitrov B, Goldman M, Nayfach S, Pollard KS. MIDAS2: Metagenomic Intra-species Diversity Analysis System. Bioinformatics. 2023;39(1). Epub 2022/11/03. doi: 10.1093/bioinformatics/btac713.
55. Almeida A, Nayfach S, Boland M, Strozzi F, Beracochea M, Shi ZJ, Pollard KS, Sakharova E, Parks DH, Hugenholtz P, Segata N, Kyrpides NC, Finn RD. A unified catalog of 204,938 reference genomes from the human gut microbiome. Nature Biotechnology. 2021;39(1):105–14. doi: 10.1038/s41587-020-0603-3.

56. Qiao J, Liang Y, Wang Y, Morigen. Trimethylamine N-Oxide Reduces the Susceptibility of Escherichia coli to Multiple Antibiotics. Front Microbiol. 2022;13:956673. Epub 2022/07/26. doi: 10.3389/fmicb.2022.956673. [PubMed: 35875516]
57. Kim HS, Nagore D, Nikaido H. Multidrug efflux pump MdtBC of Escherichia coli is active only as a B2C heterotrimer. J Bacteriol. 2010;192(5):1377–86. Epub 2009/12/30. doi: 10.1128/jb.01448-09. [PubMed: 20038594]
58. Guo H, Courbon GM, Bueler SA, Mai J, Liu J, Rubinstein JL. Structure of mycobacterial ATP synthase bound to the tuberculosis drug bedaquiline. Nature. 2021;589(7840):143–7. Epub 2020/12/11. doi: 10.1038/s41586-020-3004-3. [PubMed: 33299175]
59. Sonnenkalb L, Carter JJ, Spitaleri A, Iqbal Z, Hunt M, Malone KM, Utpatel C, Cirillo DM, Rodrigues C, Nilgiriwala KS, Fowler PW, Merker M, Niemann S. Bedaquiline and clofazimine resistance in Mycobacterium tuberculosis: an in-vitro and in-silico data analysis. Lancet Microbe. 2023;4(5):e358–e68. Epub 2023/04/02. doi: 10.1016/s2666-5247(23)00002-2. [PubMed: 37003285]
60. Sarathy JP, Ragunathan P, Shin J, Cooper CB, Upton AM, Grüber G, Dick T. TBAJ-876 Retains Bedaquiline's Activity against Subunits c and ε of Mycobacterium tuberculosis F-ATP Synthase. Antimicrob Agents Chemother. 2019;63(10). Epub 2019/07/31. doi: 10.1128/aac.01191-19.
61. Ismail N, Dippenaar A, Warren RM, Peters RPH, Omar SV. Emergence of Canonical and Noncanonical Genomic Variants following In Vitro Exposure of Clinical Mycobacterium tuberculosis Strains to Bedaquiline or Clofazimine. Antimicrobial Agents and Chemotherapy.0(0):e01368–22. doi: 10.1128/aac.01368-22.
62. Safi H, Gopal P, Lingaraju S, Ma S, Levine C, Dartois V, Yee M, Li L, Blanc L, Ho Liang H- P, Husain S, Hoque M, Soteropoulos P, Rustad T, Sherman DR, Dick T, Alland D. Phase variation in Mycobacterium tuberculosis glpK produces transiently heritable drug tolerance. Proceedings of the National Academy of Sciences. 2019;116(39):19665–74. doi: 10.1073/pnas.1907631116.
63. Bellerose MM, Baek SH, Huang CC, Moss CE, Koh EI, Proulx MK, Smith CM, Baker RE, Lee JS, Eum S, Shin SJ, Cho SN, Murray M, Sassetti CM. Common Variants in the Glycerol Kinase Gene Reduce Tuberculosis Drug Efficacy. mBio. 2019;10(4). Epub 2019/08/01. doi: 10.1128/mBio.00663-19.
64. Hards K, McMillan DGG, Schurig-Briccio LA, Gennis RB, Lill H, Bald D, Cook GM. Ionophoric effects of the antitubercular drug bedaquiline. Proceedings of the National Academy of Sciences. 2018;115(28):7326–31. doi: 10.1073/pnas.1803723115.
65. Testing TECoAS. Breakpoint tables for interpretation of MICs and zone diameters, version 10.0, 2020 2020. Available from: https://www.eucast.org/clinical_breakpoints/.
66. Pasupuleti C Investigation of the added therapeutic potential of Clofazimine in combating antimicrobial resistance in Clostridium difficile 2021.
67. Goldstein BP. Resistance to rifampicin: a review. The Journal of Antibiotics. 2014;67(9):625–30. doi: 10.1038/ja.2014.107. [PubMed: 25118103]
68. Miotto P, Cabibbe AM, Borroni E, Degano M, Cirillo DM. Role of Disputed Mutations in the rpoB Gene in Interpretation of Automated Liquid MGIT Culture Results for Rifampin Susceptibility Testing of Mycobacterium tuberculosis. J Clin Microbiol. 2018;56(5). Epub 2018/03/16. doi: 10.1128/jcm.01599-17.
69. Rando-Segura A, Aznar ML, Moreno MM, Espasa Soley M, Sulleiro Igual E, Bocanegra Garcia C, Gil Olivas E, Nindia Eugénio A, Escartin Huesca C, Zacarias A, Vegue Collado J, Katimba D, Vivas Cano MC, Gabriel E, López García MT, Pumarola Suñe T, Molina Romero I, Tórtola Fernández MT. Molecular characterization of rpoB gene mutations in isolates from tuberculosis patients in Cubal, Republic of Angola. BMC Infectious Diseases. 2021;21(1):1056. doi: 10.1186/s12879-021-06763-8. [PubMed: 34641802]
70. Boyaci H, Chen J, Lilic M, Palka M, Mooney RA, Landick R, Darst SA, Campbell EA. Fidaxomicin jams Mycobacterium tuberculosis RNA polymerase motions needed for initiation via RbpA contacts. eLife. 2018;7:e34823. doi: 10.7554/eLife.34823. [PubMed: 29480804]
71. Curry SR, Marsh JW, Shutt KA, Muto CA, O'Leary MM, Saul MI, Pasculle AW, Harrison LH. High frequency of rifampin resistance identified in an epidemic Clostridium difficile clone from a large teaching hospital. Clin Infect Dis. 2009;48(4):425–9. Epub 2009/01/15. doi: 10.1086/596315. [PubMed: 19140738]

72. Wichelhaus Thomas A, Böddinghaus B, Besier S, Schäfer V, Brade V, Ludwig A. Biological Cost of Rifampin Resistance from the Perspective of Staphylococcus aureus. Antimicrobial Agents and Chemotherapy. 2002;46(11):3381–5. doi: 10.1128/AAC.46.11.3381-3385.2002. [PubMed: 12384339]

73. Olm MR, Crits-Christoph A, Bouma-Gregson K, Firek BA, Morowitz MJ, Banfield JF. inStrain profiles population microdiversity from metagenomic data and sensitively detects shared microbial strains. Nat Biotechnol. 2021;39(6):727–36. Epub 2021/01/20. doi: 10.1038/s41587-020-00797-0. [PubMed: 33462508]

74. Kabir S, Tahir Z, Mukhtar N, Sohail M, Saqalein M, Rehman A. Fluoroquinolone resistance and mutational profile of gyrA in pulmonary MDR tuberculosis patients. BMC Pulmonary Medicine. 2020;20(1):138. doi: 10.1186/s12890-020-1172-4. [PubMed: 32393213]

75. Organization WH. Catalogue of mutations in Mycobacterium tuberculosis complex and their association with drug resistance 2021.

76. Kaushik A, Ammerman NC, Tyagi S, Saini V, Vervoort I, Lachau-Durand S, Nuermberger E, Andries K. Activity of a Long-Acting Injectable Bedaquiline Formulation in a Paucibacillary Mouse Model of Latent Tuberculosis Infection. Antimicrobial Agents and Chemotherapy. 2019;63(4):e00007–19. doi: 10.1128/AAC.00007-19. [PubMed: 30745396]

77. Rouan MC, Lounis N, Gevers T, Dillen L, Gilissen R, Raoof A, Andries K. Pharmacokinetics and pharmacodynamics of TMC207 and its N-desmethyl metabolite in a murine model of tuberculosis. Antimicrob Agents Chemother. 2012;56(3):1444–51. Epub 2011/12/14. doi: 10.1128/aac.00720-11. [PubMed: 22155815]

78. Lavelle A, Hoffmann TW, Pham HP, Langella P, Guedon E, Sokol H. Baseline microbiota composition modulates antibiotic-mediated effects on the gut microbiota and host. Microbiome. 2019;7(1):111. Epub 2019/08/04. doi: 10.1186/s40168-019-0725-3. [PubMed: 31375137]

79. Geva-Zatorsky N, Sefik E, Kua L, Pasman L, Tan TG, Ortiz-Lopez A, Yanortsang TB, Yang L, Jupp R, Mathis D, Benoist C, Kasper DL. Mining the Human Gut Microbiota for Immunomodulatory Organisms. Cell. 2017;168(5):928–43 e11. Epub 2017/02/22. doi: 10.1016/j.cell.2017.01.022. [PubMed: 28215708]

80. Skelly AN, Sato Y, Kearney S, Honda K. Mining the microbiota for microbial and metabolite-based immunotherapies. Nature Reviews Immunology. 2019;19(5):305–23. doi: 10.1038/s41577-019-0144-5.

81. Schirmer M, Garner A, Vlamakis H, Xavier RJ. Microbial genes and pathways in inflammatory bowel disease. Nature Reviews Microbiology. 2019;17(8):497–511. doi: 10.1038/s41579-019-0213-6. [PubMed: 31249397]

82. Zeng MY, Inohara N, Nuñez G. Mechanisms of inflammation-driven bacterial dysbiosis in the gut. Mucosal Immunol. 2017;10(1):18–26. Epub 2016/08/25. doi: 10.1038/mi.2016.75. [PubMed: 27554295]

83. van Duin D, Paterson DL. Multidrug-Resistant Bacteria in the Community: Trends and Lessons Learned. Infect Dis Clin North Am. 2016;30(2):377–90. doi: 10.1016/j.idc.2016.02.004. [PubMed: 27208764]

84. Carvalho MJ, Sands K, Thomson K, Portal E, Mathias J, Milton R, Gillespie D, Dyer C, Akpulu C, Boostrom I, Hogan P, Saif H, Ferreira A, Nieto M, Hender T, Hood K, Andrews R, Watkins WJ, Hassan B, Chan G, Bekele D, Solomon S, Metaferia G, Basu S, Naha S, Sinha A, Chakravorty P, Mukherjee S, Iregbu K, Modibbo F, Uwaezuoke S, Audu L, Edwin CP, Yusuf AH, Adeleye A, Mukkadas AS, Zahra R, Shirazi H, Muhammad A, Ullah SN, Jan MH, Akif S, Mazarati JB, Rucogoza A, Gaju L, Mehtar S, Bulabula ANH, Whitelaw A, Roberts L, Walsh TR, Group B. Antibiotic resistance genes in the gut microbiota of mothers and linked neonates with or without sepsis from low- and middle-income countries. Nature Microbiology. 2022;7(9):1337–47. doi: 10.1038/s41564-022-01184-y.

85. Kelly MS, Ward DV, Severyn CJ, Arshad M, Heston SM, Jenkins K, Martin PL, McGill L, Stokhuyzen A, Bhattarai SK, Bucci V, Seed PC. Gut Colonization Preceding Mucosal Barrier Injury Bloodstream Infection in Pediatric Hematopoietic Stem Cell Transplantation Recipients. Biol Blood Marrow Transplant. 2019;25(11):2274–80. Epub 2019/07/22. doi: 10.1016/j.bbmt.2019.07.019. [PubMed: 31326608]

86. Gröschel MI, Omansen TF, de Lange W, van der Werf TS, Lokate M, Bathoorn E, Akkerman OW, Stienstra Y. Multidrug-Resistant Tuberculosis Complicated by Nosocomial Infection with Multidrug-Resistant Enterobacteriaceae. Am J Trop Med Hyg. 2016;94(3):517–8. Epub 2016/01/13. doi: 10.4269/ajtmh.15-0690. [PubMed: 26755567]

87. Ravensbergen SJ, Louka C, Lokate M, Bathoorn E, Pournaras S, van der Werf TS, de Lange WCM, Stienstra Y, Akkerman OW. Case Report: Carbapenemase-Producing Enterobacteriaceae in an Asylum Seeker with Multidrug-Resistant Tuberculosis. Am J Trop Med Hyg. 2018;98(2):376–8. Epub 2017/12/28. doi: 10.4269/ajtmh.17-0544. [PubMed: 29280429]

88. Kim D-W, Cha C-J. Antibiotic resistome from the One-Health perspective: understanding and controlling antimicrobial resistance transmission. Experimental & Molecular Medicine. 2021;53(3):301–9. doi: 10.1038/s12276-021-00569-z. [PubMed: 33642573]

89. Gillespie SH, Crook AM, McHugh TD, Mendel CM, Meredith SK, Murray SR, Pappas F, Phillips PPJ, Nunn AJ. Four-Month Moxifloxacin-Based Regimens for Drug-Sensitive Tuberculosis. New England Journal of Medicine. 2014;371(17):1577–87. doi: 10.1056/NEJMoa1407426. [PubMed: 25196020]

90. Barreto HC, Gordo I. Intrahost evolution of the gut microbiota. Nature Reviews Microbiology. 2023. doi: 10.1038/s41579-023-00890-6.

91. Zhang J, Knight R. Genomic mutations within the host microbiome: Adaptive evolution or purifying selection. Engineering. 2022. doi: 10.1016/j.eng.2021.11.018.

92. Wollein Waldetoft K, Sundius S, Kuske R, Brown Sam P. Defining the Benefits of Antibiotic Resistance in Commensals and the Scope for Resistance Optimization. mBio. 2022;0(0):e01349–22. doi: 10.1128/mbio.01349-22.

93. Mortzfeld BM, Palmer JD, Bhattarai SK, Dupre HL, Mercado-Lubio R, Silby MW, Bang C, McCormick BA, Bucci V. Microcin MccI47 selectively inhibits enteric bacteria and reduces carbapenem-resistant Klebsiella pneumoniae colonization in vivo when administered via an engineered live biotherapeutic. Gut Microbes. 2022;14(1):2127633. Epub 2022/09/30. doi: 10.1080/19490976.2022.2127633. [PubMed: 36175830]

94. Hyun J, Lee SK, Cheon JH, Yong DE, Koh H, Kang YK, Kim MH, Sohn Y, Cho Y, Baek YJ, Kim JH, Ahn JY, Jeong SJ, Yeom JS, Choi JY. Faecal microbiota transplantation reduces amounts of antibiotic resistance genes in patients with multidrug-resistant organisms. Antimicrobial Resistance & Infection Control. 2022;11(1):20. doi: 10.1186/s13756-022-01064-4. [PubMed: 35093183]

95. Caballero S, Carter R, Ke X, Sušac B, Leiner IM, Kim GJ, Miller L, Ling L, Manova K, Pamer EG. Distinct but Spatially Overlapping Intestinal Niches for Vancomycin-Resistant Enterococcus faecium and Carbapenem-Resistant Klebsiella pneumoniae. PLOS Pathogens. 2015;11(9):e1005132. doi: 10.1371/journal.ppat.1005132. [PubMed: 26334306]

96. Bucci V Software: Commensal Antimicrobial Resistance Mediates Microbiome Resilience to Antibiotic Disruption 2023. doi: 10.5281/zenodo.8419675.

97. Magurran AE. Measuring biological diversity: John Wiley & Sons; 2013.

98. Sonnenkalb L, Carter JJ, Spitaleri A, Iqbal Z, Hunt M, Malone KM, Utpatel C, Cirillo DM, Rodrigues C, Nilgiriwala KS, Fowler PW, Merker M, Niemann S, Comprehensive Resistance Prediction for Tuberculosis: an International C. Bedaquiline and clofazimine resistance in Mycobacterium tuberculosis: an in-vitro and in-silico data analysis. Lancet Microbe. 2023;4(5):e358–e68. Epub 20230329. doi: 10.1016/S2666-5247(23)00002-2. [PubMed: 37003285]

99. Walsh KM KF, Lee MH, Vilbrun SC, Mathurin L, Jean Francois D, Zimmerman, Kaya F, Zhang N, Saito K, Ocheretina O, Savic R, Dartois V, Johnson WD, Pape JW, Nathan C, Fitzgerald DW. Early bactericidal activity trial of nitazoxanide for pulmonary tuberculosis. Antimicrobial Agents and Chemotherapy. 2020. Epub 2020 Feb 18. doi: 10.1128/AAC.01956-19.

100. Diacon AH, van der Merwe L, Demers AM, von Groote-Bidlingmaier F, Venter A, Donald PR. Time to positivity in liquid culture predicts colony forming unit counts of Mycobacterium tuberculosis in sputum specimens. Tuberculosis (Edinb). 2014;94(2):148–51. Epub 2014/01/25. doi: 10.1016/j.tube.2013.12.002. [PubMed: 24456754]

101. Harris PA, Taylor R, Thielke R, Payne J, Gonzalez N, Conde JG. Research electronic data capture (REDCap)--a metadata-driven methodology and workflow process for providing

translational research informatics support. J Biomed Inform. 2009;42(2):377–81. doi: 10.1016/j.jbi.2008.08.010. [PubMed: 18929686]

102. Wipperman MF, Fitzgerald DW, Juste MAJ, Taur Y, Namasivayam S, Sher A, Bean JM, Bucci V, Glickman MS. Antibiotic treatment for Tuberculosis induces a profound dysbiosis of the microbiome that persists long after therapy is completed. Sci Rep. 2017;7(1):10767. doi: 10.1038/s41598-017-10346-6. [PubMed: 28883399]
103. Dupnik KM, Bean JM, Lee MH, Jean Juste MA, Skrabanek L, Rivera V, Vorkas CK, Pape JW, Fitzgerald DW, Glickman M. Blood transcriptomic markers of Mycobacterium tuberculosis load in sputum. Int J Tuberc Lung Dis. 2018;22(8):950–8. doi: 10.5588/ijtld.17.0855 10.5588/ijtld.17.0855. PubMed PMID: 29991407; PMCID: 6343854. [PubMed: 29991407]
104. Dobin A, Davis CA, Schlesinger F, Drenkow J, Zaleski C, Jha S, Batut P, Chaisson M, Gingeras TR. STAR: ultrafast universal RNA-seq aligner. Bioinformatics. 2012;29(1):15–21. doi: 10.1093/bioinformatics/bts635. [PubMed: 23104886]
105. Liao Y, Smyth GK, Shi W. featureCounts: an efficient general purpose program for assigning sequence reads to genomic features. Bioinformatics (Oxford, England). 2014;30(7):923–30. doi: 10.1093/bioinformatics/btt656. [PubMed: 24227677]
106. Hartley SW, Mullikin JC. QoRTs: a comprehensive toolset for quality control and data processing of RNA-Seq experiments. BMC bioinformatics. 2015;16(1):224-. doi: 10.1186/s12859-015-0670-5. [PubMed: 26187896]
107. Mallick H, Rahnavard A, McIver LJ, Ma S, Zhang Y, Nguyen LH, Tickle TL, Weingart G, Ren B, Schwager EH, Chatterjee S, Thompson KN, Wilkinson JE, Subramanian A, Lu Y, Waldron L, Paulson JN, Franzosa EA, Bravo HC, Huttenhower C. Multivariable association discovery in population-scale meta-omics studies. PLOS Computational Biology. 2021;17(11):e1009442. doi: 10.1371/journal.pcbi.1009442. [PubMed: 34784344]
108. Ritchie ME, Phipson B, Wu D, Hu Y, Law CW, Shi W, Smyth GK. limma powers differential expression analyses for RNA-sequencing and microarray studies. Nucleic Acids Res. 2015;43(7):e47–e. Epub 2015/01/20. doi: 10.1093/nar/gkv007. [PubMed: 25605792]
109. Barbie DA, Tamayo P, Boehm JS, Kim SY, Moody SE, Dunn IF, Schinzel AC, Sandy P, Meylan E, Scholl C, Frohling S, Chan EM, Sos ML, Michel K, Mermel C, Silver SJ, Weir BA, Reiling JH, Sheng Q, Gupta PB, Wadlow RC, Le H, Hoersch S, Wittner BS, Ramaswamy S, Livingston DM, Sabatini DM, Meyerson M, Thomas RK, Lander ES, Mesirov JP, Root DE, Gilliland DG, Jacks T, Hahn WC. Systematic RNA interference reveals that oncogenic KRAS-driven cancers require TBK1. Nature. 2009;462(7269):108–12. Epub 2009/10/23. doi: 10.1038/nature08460. [PubMed: 19847166]
110. Liberzon A, Birger C, Thorvaldsdottir H, Ghandi M, Mesirov JP, Tamayo P. The Molecular Signatures Database (MSigDB) hallmark gene set collection. Cell Syst. 2015;1(6):417–25. Epub 2016/01/16. doi: 10.1016/j.cels.2015.12.004. [PubMed: 26771021]
111. Hanzelmann S, Castelo R, Guinney J. GSVA: gene set variation analysis for microarray and RNA-seq data. BMC Bioinformatics. 2013;14:7. Epub 2013/01/18. doi: 10.1186/1471-2105-14-7. [PubMed: 23323831]
112. Dsouza M, Menon R, Crossette E, Bhattarai SK, Schneider J, Kim Y-G, Reddy S, Caballero S, Felix C, Cornacchione L, Hendrickson J, Watson AR, Minot SS, Greenfield N, Schopf L, Szabady R, Patarroyo J, Smith W, Harrison P, Kuijper EJ, Kelly CP, Olle B, Bobilev D, Silber JL, Bucci V, Roberts B, Faith J, Norman JM. Colonization of the live biotherapeutic product VE303 and modulation of the microbiota and metabolites in healthy volunteers. Cell Host & Microbe. 2022;30(4):583–98.e8. doi: 10.1016/j.chom.2022.03.016. [PubMed: 35421353]
113. Zhao C, Dimitrov B, Goldman M, Nayfach S, Pollard KS. MIDAS2: Metagenomic Intra-species Diversity Analysis System. bioRxiv. 2022:2022.06.16.496510. doi: 10.1101/2022.06.16.496510.
114. Kursa MB, Rudnicki WR. Feature Selection with the Boruta Package. 2010. 2010;36(11):13. Epub 2010–08-05. doi: 10.18637/jss.v036.i11.
115. Pettersen EF, Goddard TD, Huang CC, Meng EC, Couch GS, Croll TI, Morris JH, Ferrin TE. UCSF ChimeraX: Structure visualization for researchers, educators, and developers. Protein Sci. 2021;30(1):70–82. Epub 20201022. doi: 10.1002/pro.3943. [PubMed: 32881101]

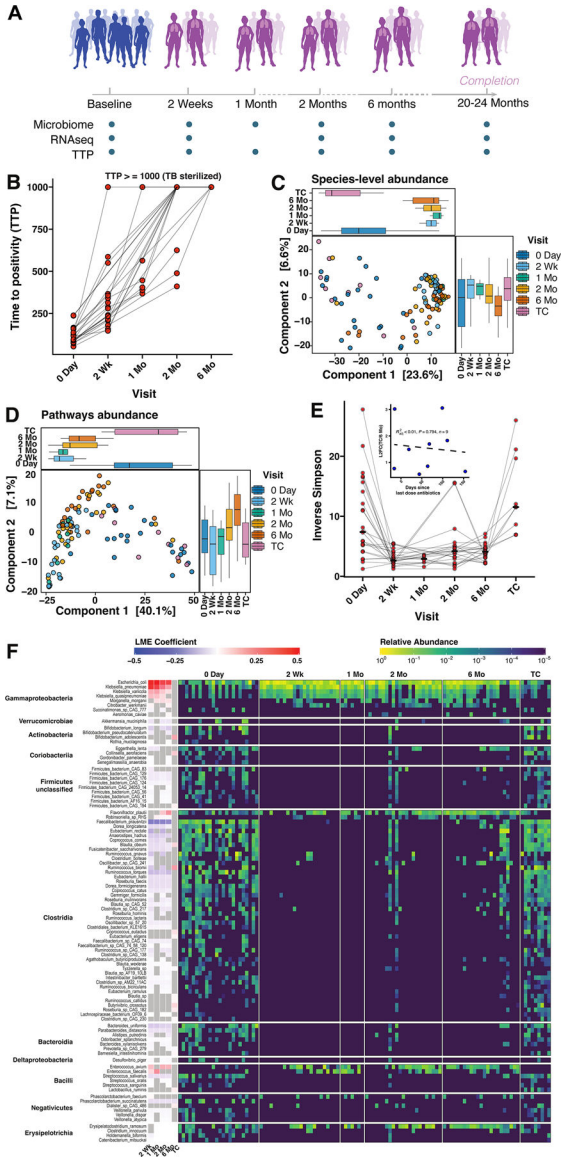

Fig. 1. MDR TB treatment induces Mtb lung sterilization and causes a temporary perturbation in the microbiome, which recovers by treatment cessation.

A. Schematic of the MDR TB treatment observational cohort. **B.** Time to positivity (TTP) was measured at baseline (day 0), 2 weeks, 1 month, 2 months, 6 months during treatment, and at treatment cessation (TC) (20–24 months). **C to D.** Principal Coordinate Analysis on center-log-ratio transformed data for species abundances (C) and functional pathway abundance (D) from metagenomic sequencing. **E.** Microbiome diversity was computed for each study volunteer at the different time points and quantified using the inverse Simpson index(97). Linear regression modeling (inset) was used to predict fold-change in diversity occurring between 6 months and treatment completion as a function of time from antibiotic cessation. **F.** Taxonomic abundance of the microbiome during MDR treatment. The annotations to the right of the bacterial names indicate whether a species was significantly perturbed (FDR < 0.05) by treatment at any time point compared to baseline (Day 0) with red indicating enrichment and blue indicating depression in abundance. Grey

indicates not significant. Heatmap columns are split by time point membership (including baseline), and rows by phylogenetic order.

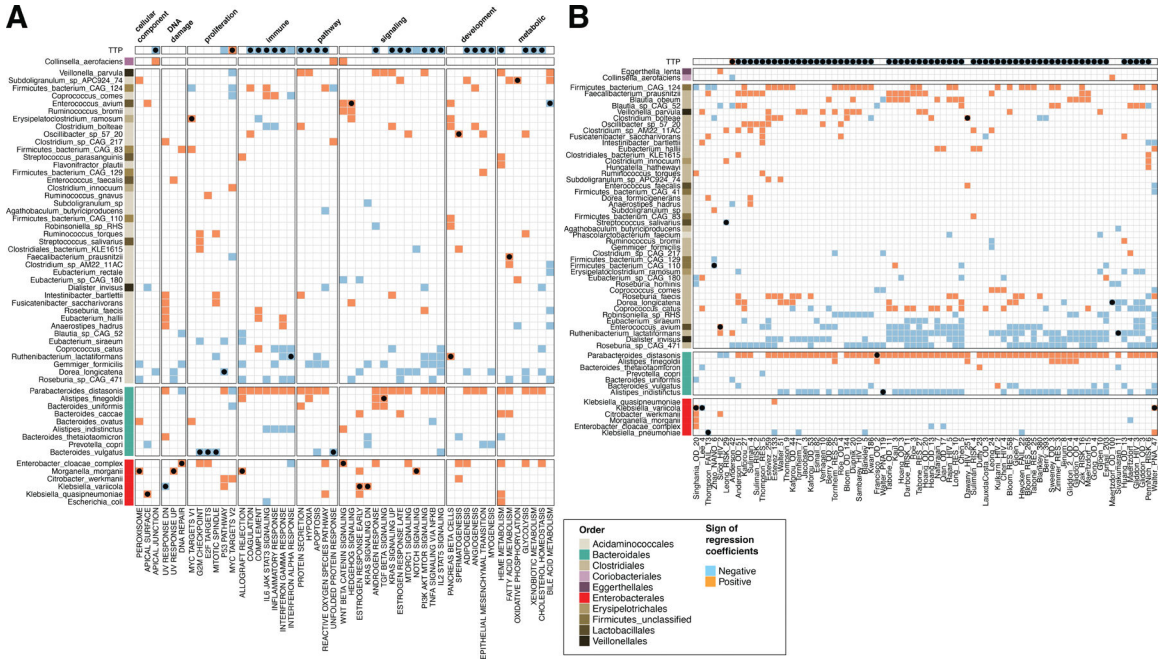

Fig. 2. Resolution of TB disease state as a function of microbiome perturbation and pathogen killing.

Mixed-effects Random Forest Regression Modeling was run to predict the normalized enrichment score (NES) of **A.** MSigDB hallmark pathways or **B.** TB-associated gene signatures. Permutated importance analysis was used to identify features (both microbiome species and TTP) significantly associated (FDR < 0.1) with each modeled peripheral transcriptional signature. We then used univariate linear mixed-effects models to determine directionality of the associations; blue indicates a negative relationship, and red a positive one. The black dot indicates the strongest predictor for that specific hallmark pathway or TB-associated gene signature.

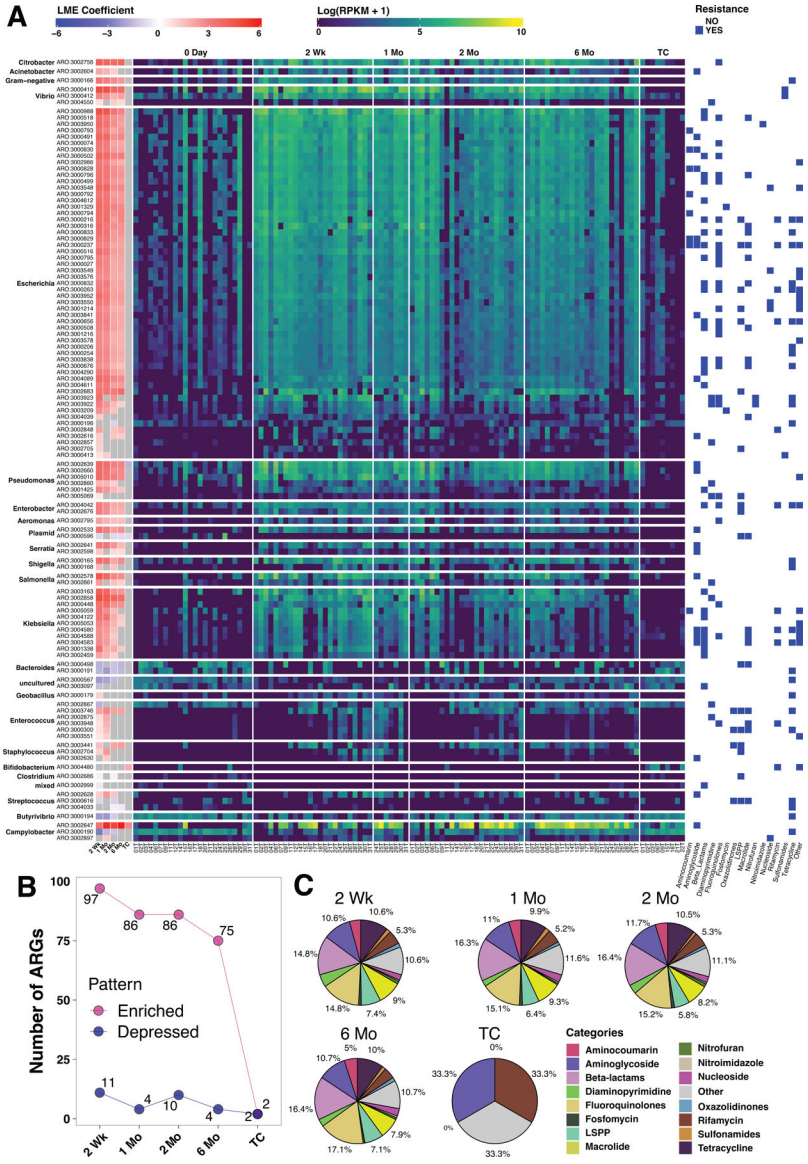

Fig. 3. MDR TB therapy enriches antimicrobial resistance across drug classes.

A database of antibiotic resistance gene (ARGs) marker sequences from the 2021 CARD database was built using ShortBRED. Shotgun metagenomic data were mapped against this marker database and profiled for the abundance of ARGs. Linear mixed-effects modeling was run to determine whether ARGs were significantly enriched or depressed at treatment points compared to baseline (day 0). **A.** Heatmap of treatment-affected ARGs. Row annotation represents the value of the regression coefficient. Red = significantly (FDR < 0.05) enriched, blue = significantly (FDR < 0.05) repressed, and grey = not significantly different (FDR > 0.05). The heatmap represents ARGs abundance in each sample quantified as logarithm of the Reads Per Kilobase per Million (Log(RPKM+1)) mapped reads for each ARG. **B.** Quantification of the total number of ARGs enriched or repressed compared to baseline. **C.** Pie charts representing the frequency of resistance class for the ARGs significantly affected by MDR TB treatment at different time points.

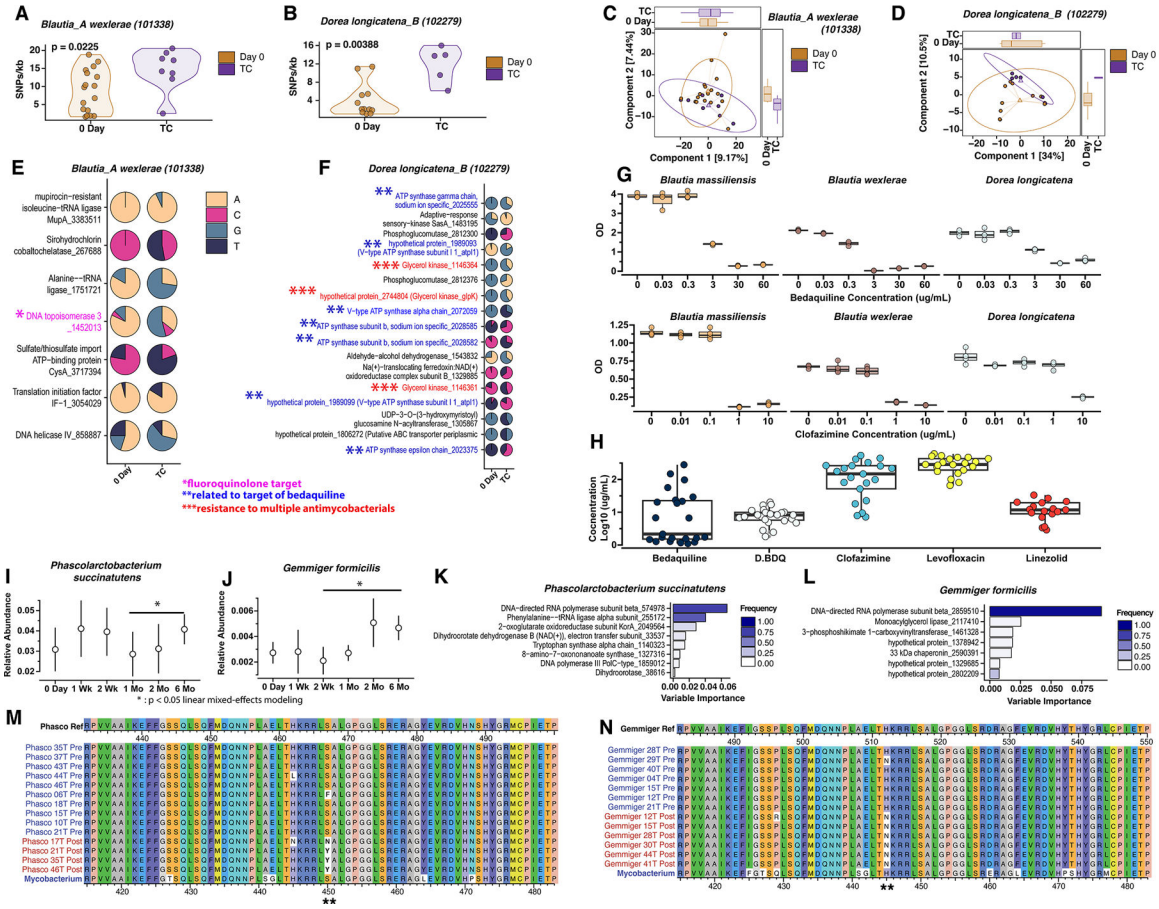

Fig. 4. Microbiome resilience corresponds to the emergence of antimicrobial resistance in commensals.

(**A-D**) Allelic composition of *B. wexlerae A* and *D. longicatena B* core genomes (with respect to the reference) in treatment cessation and baseline samples. **A.** and **B.** SNPs diversity distribution (SNPs/kilobase compared to reference for *B. wexlerae A* and *D. longicatena B.* **C.** and **D.** Ordination analysis of core genome allele frequencies. **E.** and **F.** Random Forest Classification Modeling. For every genetic feature, the distribution of the minor allele DNA nucleotide for each SNP is shown. The numeric value next to gene name is the SNP position in the reference genome (Site ID). Asterisk indicates genes that are known to be related to the mechanism of action or resistance to drugs contained in the MDR TB treatment cocktail. The MIDAS-reported ATP synthase indicates the eubacterial F-type ATP synthase, whereas the MIDAS-reported V-type ATP synthase refers to the eubacterial V/A ATPase. **G.** Bedaquiline and clofazimine are active against anaerobic commensals *in vitro.* The axis shows optical density of liquid cultures at different drug concentrations on the X axis. **H.** Quantitation of bedaquiline, desmethyl bedaquiline (D.BDQ), clofazimine, levofloxacin, and linezolid from stool samples at 6 months of treatment with drug concentration given on a log scale in ug/ml. **I to J.** The abundance of (**I**) *P. succinatutens* and (**J**) *G. formicilis* during HRZE therapy showing depletion and recovery as median +/− mean absolute deviation. **K** and **L**. Random Forest Classification on MIDAS data identifies SNPs in the *Phascolarctobacterium* (K) or *Gemminger* (L) RNA polymerase

beta subunit, the direct molecular target of rifampin (R), as the strongest predictor of treatment time. **M.** and **N.** Amino acid sequence alignments for baseline and 6-month HRZE samples highlighting mutations S450Y and H445N detected in treatment completion (post) vs. pretreatment samples. The *Phascolarctobacterium* (**M**) or *Gemminger* (**N**) reference RpoB sequences are displayed above the alignment. The *M. tuberculosis* RpoB sequence is shown below. Mutation positions are marked with **.

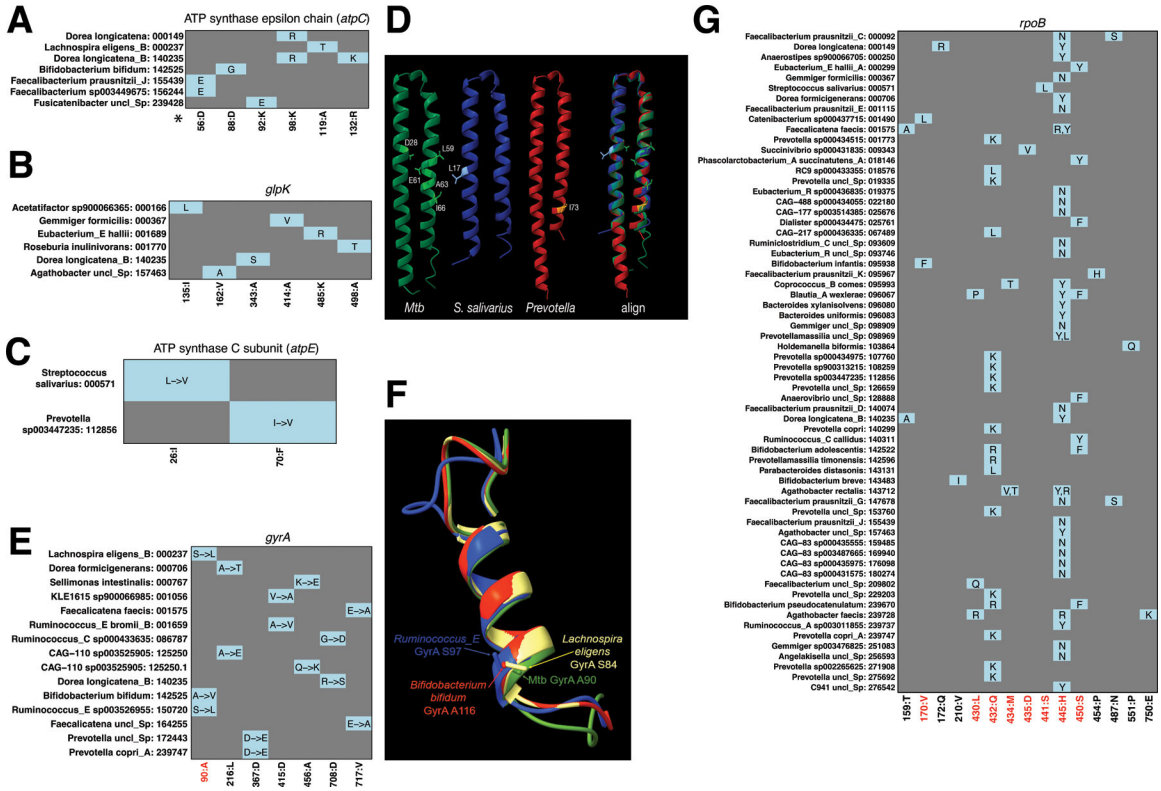

Fig. 5: Evolution of widespread commensal resistance under antibiotic pressure.

Mutations detected by inStrain in the microbiomes of MDR-treated subjects, including in ATP synthase subunit epsilon **(A),** *glpK*, **(B)**, *atpE* **(C)**, and *gyrA* **(E)**. For each panel, the amino acid positions in the *M. tuberculosis* protein were determined by inStrain where red shading indicates a position of resistance mutations in *M. tuberculosis* according to (75). **D.** *M. tuberculosis* C subunit *(atpE)* was modeled by AlphaFold from Uniprot ID P9WPS1 in green. Positions of mutations in *atpE* associated with bedaquiline resistance were taken from(98) and are shown with amino acid side chains in light green (wild type AA). The *S. salivarius* (blue, Uniprot ID A0A413AC39) and *Prevotella* (red, Uniprot ID A0A3C1E6Z4) *atpE* encoded proteins were predicted using AlphaFold and the positions of the inStrain detected mutations are shown in lighter color than the backbone helix with side chains of the wild type AA shown. The three structures were aligned using the Matchmaker function of ChimeraX. **F.** Structural modeling of *gyrA* mutations uses *M. tuberculosis* GyrA (green, PDB 3IFZ), *Ruminococcus E* GyrA (Blue, AlphaFold prediction from Uniprot ID A0A7J5TQ36), *Bifidobacterium bifidum* (red, AlphaFold prediction from Uniprot ID A0A7J5TQ36), and *Lachnospira eligens* (yellow, AlphaFold prediction from Uniprot ID A0A415M9D7). Only the alignment from AA H85-P108 of Mtb GyrA is shown with the positions of Mtb GyrA A90 and detected mutation positions shown with side chains. **G.** Widespread RpoB mutations in the microbiomes of subjects treated with standard TB therapy (HRZE).

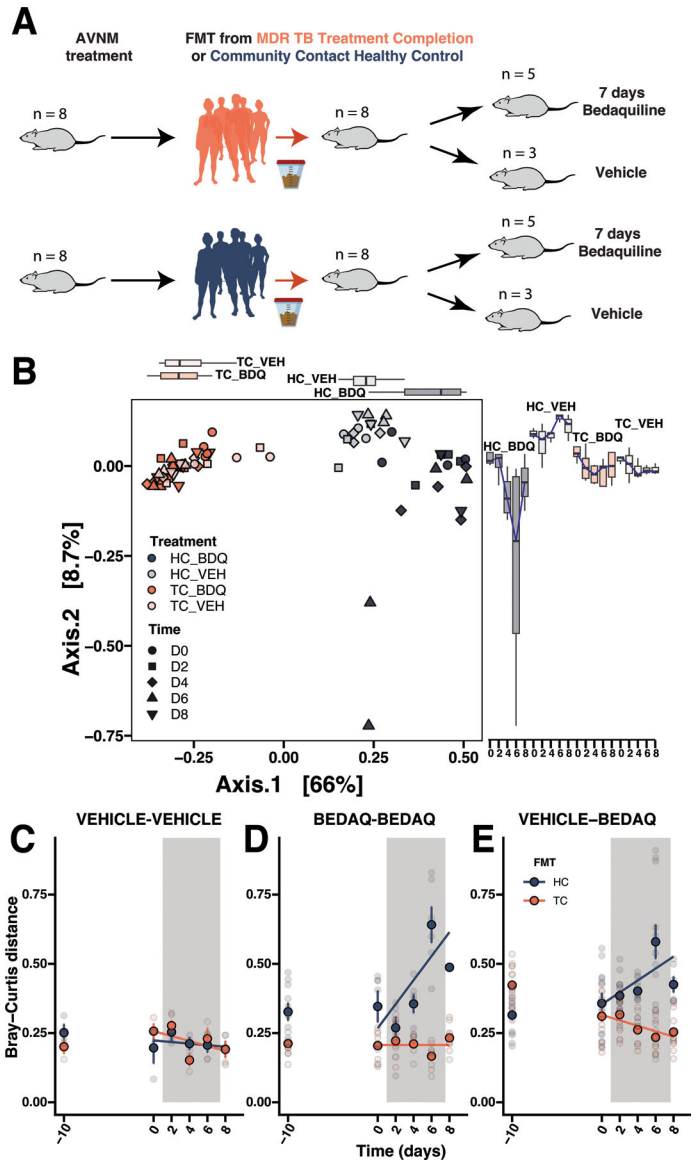

Fig. 6. MDR TB treatment completion microbiome is desensitized to bedaquiline rechallenge.

A. We performed adoptive microbiome transfer experiments wherein AVNM-pre-treated mice were orally gavaged with a fecal matter transplant (FMT) from MDR TB treatment completion (TC) individuals or healthy community contact controls (HC), before receiving 7 consecutive days of bedaquiline or vehicle via oral gavage. Biologic replicate numbers are shown. **B.** Principal Component Analysis performed on the Bray-Curtis distance among samples. Samples are colored based on FMT, with shapes corresponding to different treatment days. **C-E.** We tested the hypothesis that the distance in microbiome composition between AVNM-treated mice receiving a fecal matter transplant (FMT) from MDR TB treatment completion (TC) individuals and challenged with 7 days of bedaquiline or vehicle is smaller than the distance in mice that received FMT from healthy community controls and administered with bedaquiline or vehicle. Linear-mixed effects modeling to predict the Bray-Curtis distance as a function of time since bedaquiline initiation, FMT type (HC/TC),

antibiotic type (bedaquiline/vehicle) alone as well as their interaction was fit to the distances between **C**. every vehicle sample to every other vehicle sample, **D.** every bedaquiline sample to every other vehicle bedaquiline samples, and **E.** every vehicle sample to every bedaquiline sample.